Research Paper

The caloric value of food intake structurally adjusts a neuronal mushroom body circuit mediating olfactory learning in *Drosophila*

Büşra Çoban,[1] Haiko Poppinga,[1] El Yazid Rachad,[1] Bart Geurten,[2] David Vasmer,[1] Francisco Jesus Rodriguez Jimenez,[3] Yogesh Gadgil,[1] Stephan Hubertus Deimel,[1] Idan Alyagor,[4] Oren Schuldiner,[4] Ilona C. Grunwald Kadow,[3] Thomas Dieter Riemensperger,[1] Annekathrin Widmann,[1] and André Fiala[1]

[1]*Molecular Neurobiology of Behavior, University of Göttingen, 37077 Göttingen, Germany;* [2]*Department of Zoology, Otago University, Dunedin 9016, New Zealand;* [3]*Faculty of Medicine, Institute of Physiology, University of Bonn, 51335 Bonn, Germany;* [4]*Department of Molecular Cell Biology, Department of Molecular Neuroscience, Weizmann Institute of Science, Rehovot 7610001, Israel*

Associative learning enables the adaptive adjustment of behavioral decisions based on acquired, predicted outcomes. The valence of what is learned is influenced not only by the learned stimuli and their temporal relations, but also by prior experiences and internal states. In this study, we used the fruit fly *Drosophila melanogaster* to demonstrate that neuronal circuits involved in associative olfactory learning undergo restructuring during extended periods of low-caloric food intake. Specifically, we observed a decrease in the connections between specific dopaminergic neurons (DANs) and Kenyon cells at distinct compartments of the mushroom body. This structural synaptic plasticity was contingent upon the presence of allatostatin A receptors in specific DANs and could be mimicked optogenetically by expressing a light-activated adenylate cyclase in exactly these DANs. Importantly, we found that this rearrangement in synaptic connections influenced aversive, punishment-induced olfactory learning but did not impact appetitive, reward-based learning. Whether induced by prolonged low-caloric conditions or optogenetic manipulation of cAMP levels, this synaptic rearrangement resulted in a reduction of aversive associative learning. Consequently, the balance between positive and negative reinforcing signals shifted, diminishing the ability to learn to avoid odor cues signaling negative outcomes. These results exemplify how a neuronal circuit required for learning and memory undergoes structural plasticity dependent on prior experiences of the nutritional value of food.

[Supplemental material is available for this article.]

The question of which internal and environmental factors determine the ability to learn and memorize in animals, including humans, has been a subject of intense investigation for decades (Kandel et al. 2014; Josselyn and Tonegawa 2020). A significant challenge in understanding this matter concerns the impact of an individual's past experiences on future memory acquisition and retention. Prolonged exposure to positive, negative, or even neutral experiences can profoundly influence learning abilities and the content and valence of acquired memories. To control for this complexity, researchers often turn to controlled laboratory conditions, using classical Pavlovian conditioning. In the experimental paradigm pioneered by Pavlov (1927), relatively neutral stimuli are systematically associated with either positive, rewarding cues or negative, punitive cues. This methodology allows for the efficient exploration of how effectively positive or negative predictions are formed through learning, with a focus on the dependence on previous treatment or experiences.

One factor that can significantly impact learning and memory formation is the sustained experience of either constant oversaturation with food rich in calories or enduring permanent hunger due to low-caloric food. The connection between nutrition, feeding behavior, and learning involves multiple, intricately related factors. For instance, protein-synthesis-dependent long-term memory formation has been shown to be contingent on a high-caloric content, as evidenced by studies on both larval and adult fruit flies (Plaçais et al. 2017; Eschment et al. 2020; de Tredern et al. 2021), as well as rodents (Suzuki et al. 2011; Steinman et al. 2016). In contrast, it has been reported that mild caloric restriction can enhance aversive long-term memory formation in flies (Hirano et al. 2013) and contribute to long-term memory persistence in mice (Talhati et al. 2014), and the cellular mechanisms underlying these phenomena have been described. Beyond these cellular aspects of calorie intake on memory formation, the relationship between a sensory food experience and its rewarding properties is also directly linked to learning. Extensive studies in mammals, including humans, and flies have explored how learning about food-related cues, their caloric contents, and their rewarding properties can influence food uptake and energy balance (Benoit et al. 2010; Davidson et al. 2014; Pardo-Garcia et al. 2023). In our

Corresponding author: afiala@gwdg.de
Published by Cold Spring Harbor Laboratory Press; ISSN 1549-5485/24
Article is online at http://www.learnmem.org/cgi/doi/10.1101/lm.053997.124.
Freely available online through the *Learning & Memory* Open Access option.

research, we addressed a different question, investigating how prolonged exposure to either a low- or high-caloric food experience might influence the brain's ability for associative learning and valence of the acquired knowledge. Our primary goal was to discern whether the neuronal circuits responsible for mediating associative learning related to odor cues undergo adaptive reconfiguration in both structure and function over extended periods of low- or high-caloric food intake.

Drosophila melanogaster is an excellent model organism for this investigation due to its experimental accessibility, relatively small nervous system, and simultaneously rich and intricate behavioral repertoire and learning capabilities. In our study, we specifically focus on adaptive plasticity occurring in the mushroom body of the *Drosophila* brain. This focus is motivated by the fact that the neuronal circuits within the mushroom body, which govern both appetitive and aversive odor learning, are well characterized (Heisenberg 2003; Fiala 2007; Boto et al. 2020; Menzel 2022). In *Drosophila*, the plastic changes in synaptic transmission that mediate olfactory associative learning, as well as the points of convergence between odor signals and reinforcing punishment or reward, are localized to the axonal presynapses of Kenyon cells (KCs), the intrinsic neurons of the mushroom bodies (Heisenberg 2003; Gerber et al. 2004; Aso et al. 2014b; Hige et al. 2015; Owald et al. 2015; Hancock et al. 2022).

The mushroom body of the insect brain is a complex, multifunctional, central neuronal circuit that plays a key role in the experience-dependent adaptive adjustment of behavior (for review, see Davis 1993; Heisenberg 2003; Fiala 2007; Busto et al. 2010; Boto et al. 2020; Menzel 2022). The mushroom body is also implicated in the adaptive regulation of sleep (Joiner et al. 2006; Sitaraman et al. 2015; Driscoll et al. 2021) and food uptake or foraging dependent on the internal hunger/satiation state (Al-Anzi and Zinn 2018; Tsao et al. 2018; Grunwald Kadow 2019; Sayin et al. 2019; Senapati et al. 2019). External sensory information, such as olfactory or visual signals, provides one source of input to KCs, predominantly through their dendritic input regions in the mushroom body calyx. The ∼2000 KCs encode this information as sparsely distributed activity of distinct ensembles of neurons (Turner et al. 2008; Honegger et al. 2011; Bilz et al. 2020). Three principal types of KCs (α/β, α′/β′, and γ-KCs) collectively form the mushroom body lobes with their parallel axons: The axons of α/β KCs bifurcate and form the vertical α- and horizontal β-lobes, the equally bifurcating α′/β′ KCs form the adjacent vertical α′- and horizontal β′-lobes, and the γ-KCs form the horizontal γ-lobes (Crittenden et al. 1998). Mushroom body output neurons (MBONs) arborize their dendrites in the calyx and in spatially confined compartments along the axons (Ito et al. 1998; Tanaka et al. 2008; Aso et al. 2014a). Some MBONs influence goal-directed behavior, like attraction toward or repulsion from a stimulus source (Aso et al. 2014a). For example, MBONs innervating compartments 1 and 2 of the γ-lobes mediate attraction toward the source of their own activation (Aso et al. 2014a). Conversely, MBONs innervating compartments 4 and 5 mediate repulsion from it (Aso et al. 2014a). The behavioral roles of MBONs innervating the centrally located compartment 3 of the γ-lobe are less well understood, although it has been shown that their optogenetic activation induces approach behavior toward the light source (Aso et al. 2014a), and they are required for appetitive learning (Stahl et al. 2022). In addition, modulatory neurons releasing biogenic amines, such as dopamine, octopamine, and serotonin, inhibitory transmitters such as GABA, or diverse neuropeptides innervate the mushroom body densely. The functions of multiple dopaminergic neurons (DANs) have been dissected in recent years (for review, see Kaun and Rothenfluh 2017). For example, the DANs of the protocerebral posterior lateral 1 (PPL1) cluster that innervate the γ1 and γ2 compartments mediate the reinforcing properties of punishment during associative learning (Riemensperger et al. 2005; Aso et al. 2012, 2014b). Conversely, DANs of the protocerebral anterior medial (PAM) cluster that innervate compartments 4 and 5 of the γ-lobes signal reward (Liu et al. 2012). The role of PAM-cluster DANs innervating the γ3 compartment in associative learning is less well understood. However, Yamagata et al. (2016) figured out that these neurons become inhibited by rewarding sugar stimuli, and artificially activating them can induce aversive learning; conversely, their suppression induces appetitive learning.

Here, we report that caloric restriction for a sustained period of several days causes a small group of PAM-cluster DANs that innervate the γ3, γ4, and β′1 compartments to structurally decrease their synaptic connectivity with KCs. This effect could be optogenetically induced and mimicked. Surprisingly, appetitive, reward-based learning was not affected by this structural modification. Rather, aversive, punishment-based learning was reduced. This synaptic change caused a shift in the balance between aversive and appetitive learning in a conflicting situation, ultimately leading to a reduced acquisition of repulsion.

Results

Connectivity between specific dopaminergic neurons and Kenyon cells decreases with low-caloric food

To investigate the impact of sustained exposure to low- or high-caloric foods on brain circuitry, we raised flies on a standard cornmeal medium until 3 d after eclosion, at which point their adult brains were largely developed. Following this initial period, three distinct groups of flies were separated and assigned to food treatments with varying nutritional contents and caloric values, referred to as hypocaloric, isocaloric, and hypercaloric (Fig. 1A,B). This dietary intervention persisted for 7 d. The caloric values of the different food types were chosen such that the extended exposition of the flies modified subsequent feeding-related behavior. Notably, flies exposed to hypocaloric food exhibited a significant increase in food uptake, as measured by both a capillary feeder assay (Ja et al. 2007) and an electronically controlled "FlyPad" assay (Supplemental Fig. S1A–C; Itskov et al. 2014). Moreover, the sugar-evoked proboscis extension reflex (Supplemental Fig. S1D) and odor-driven exploratory behavior (Supplemental Fig. S1E,F) were influenced by the caloric content of the food, showing enhancement in flies exposed to hypocaloric conditions. Survival rates displayed a slight decrease in flies subjected to hypo- and hypercaloric diets over an extended period compared to flies in optimized standard food or isocaloric conditions (Supplemental Fig. S2A). However, at the time of anatomical or behavioral experiments (conducted 7 d after transfer to modified food conditions or 10 d after eclosion), no significant differences in survival rates were observed between the three food types (Supplemental Fig. S2B).

We investigated the modifiability of neuronal circuit connections under different, extended feeding conditions, with a specific focus on DANs that innervate the mushroom body. We used the GFP reconstitution across synaptic partners (GRASP) technique, involving the reconstitution of complementary, membrane-bound splitGFP proteins (Feinberg et al. 2008; Gordon and Scott 2009), to quantitatively assess physical contacts in close proximity between KCs and DANs in response to different feeding conditions. One part of the membrane-bound splitGFP and a cytosolic red fluorescent marker were expressed in KCs; the second part of the membrane-bound splitGFP was under Gal4–UAS control in distinct populations of DANs (Fig. 1C; Pech et al. 2013). This approach can be used to visualize points of close physical proximity between neurons, as it is the case at synaptic connections, and to quantify

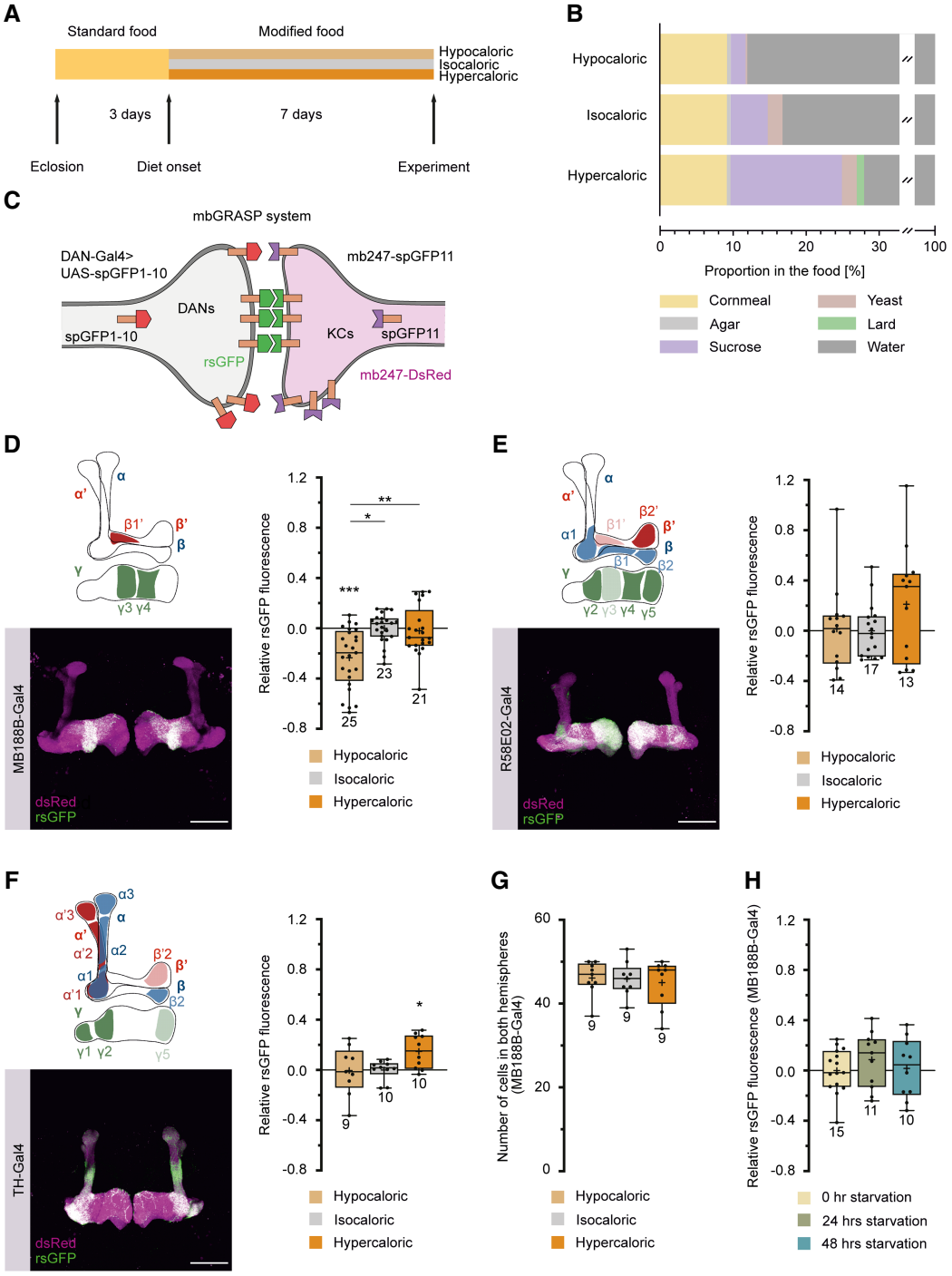

Figure 1. Calorie restriction affects the connectivity between specific dopaminergic neurons (DANs) and Kenyon cells (KCs). (*A*) Experimental time line. Flies were raised on standard food and transferred to fresh standard food after eclosion. Three days after eclosion, flies were transferred to the food of equivalent (isocaloric), lower (hypocaloric), or higher (hypercaloric) caloric value for 7 d. (*B*) Composition of hypo-, iso-, and hypercaloric food. Each food type contained agar, cornmeal, sucrose, and yeast. The hypercaloric food contained lard in addition as a source of calories. Detailed food compositions are described in the Materials and Methods section. (*C*) Visualization of the close proximity between DANs, determined by specific Gal4 lines, and KCs using reconstitution of splitGFP (rsGFP). All KCs are additionally labeled through DsRed expression. (*D–F*) Visualization and quantification of rsGFP fluorescence intensity between populations of DANs and KCs. DANs labeled by MB188B-Gal4 (*D*), R58E02-Gal4 (*E*), and TH-Gal4 (*F*) innervate the lobes of the mushroom body (magenta) in a largely complementary manner. The schematic illustrations indicate the predominantly innervated regions of the mushroom body lobes. Representative anatomical images show DsRed expression in KCs and rsGFP. Scale bar, 50 µm. The quantification of relative rsGFP fluorescence, normalized to the mean values for isocaloric food, in flies exposed to the different food conditions show that relative GFP reconstitution between MB188B-Gal4-driven DANs and KCs decreases under hypocaloric conditions (*D*), but not between R58E02-Gal4-driven (*E*) or TH-Gal4-driven (*F*) DANs. (*G*) Quantification of MB188B-Gal4-positive neurons under hypo-, iso-, and hypercaloric conditions using GCaMP3 expression as a marker. (*H*) Quantification of relative rsGFP fluorescence between MB188B-Gal4-driven DANs and KCs, normalized to the mean values for isocaloric food, in flies that were deprived of food for 0, 24, or 48 h. Box plots indicate 25/75 percentiles, lines represent medians, whiskers represent min/max values, pluses represent means, dots represent individual data points, and numbers represent sample sizes. Statistically significant deviations from the baseline are indicated as asterisks above the boxes. Statistically significant differences between groups are indicated with asterisks and lines above boxes. For statistical tests, see Supplemental Tables S1–S4. (*) $P<0.05$, (**) $P<0.01$, (***) $P<0.001$.

through fluorescence intensity the spatial extent and density of these physical contacts. It does not per se identify functional synaptic connections, but it allows us to compare physical contacts in differentially treated animals. Our findings revealed a significant reduction in contacts between KCs and a specific population of DANs, as labeled by the split-Gal4 line MB188B-Gal4 (Aso et al. 2014b), when the animals were maintained on hypocaloric food (Fig. 1D). These DANs are part of the PAM cluster and innervate the γ3 and β′1 compartments, and also the γ4 compartment of the mushroom body to a slight extent. This effect was not observed when splitGFP reconstitution between the majority of PAM-cluster DANs and KCs was analyzed (using the driver line R58E02-Gal4) (Fig. 1E; Liu et al. 2012), or between the majority of PPL1-cluster DANs and KCs (using the driver line TH-Gal4) (Fig. 1F; Friggi-Grelin et al. 2003). Rather, the connections between PPL1-cluster DANs and KCs were enhanced under hypercaloric conditions (Fig. 1F). Moreover, the decrease in splitGFP reconstitution in hypocaloric conditions in MB188B-Gal4-positive neurons was not due to a decrease in cell numbers (Fig. 1G), indicating that in fact putative synaptic connections decrease. The reduction in reconstituted splitGFP fluorescence between these DANs and KCs was not restricted to a particular mushroom body compartment, but was observed in all three compartments innervated by these DANs (Supplemental Fig. S3). However, it required exposing the animals to low-caloric food for a sustained period of several days to achieve the decrease in reconstituted splitGFP fluorescence, because starvation for 24 or 48 h by depriving the animals completely from food did not induce an equivalent effect (Fig. 1H). Subsequently, we restricted our focus on PAM-cluster DANs targeted by the MB188B-Gal4 strain.

The caloric value of food modifies the balance between reward learning and punishment learning in a conflicting situation

DANs that innervate the γ-lobes of the mushroom bodies play a crucial role in mediating reinforcing valence signals in associative olfactory learning. Specifically, the PPL1-cluster DANs that innervate compartments γ1 and γ2 are implicated in associating punishing electric shock stimuli with odors in an aversive Pavlovian conditioning paradigm, whereas the DANs of the PAM cluster that innervate compartments γ4 and γ5 mediate rewarding sugar stimuli in an appetitive conditioning paradigm (Riemensperger et al. 2005; Aso et al. 2012, 2014b; Liu et al. 2012). The role of PAM-cluster DANs innervating the central γ3 compartment appears to be a dual, balancing one, as activating them induces aversive learning and suppressing them substitutes for reward (Yamagata et al. 2016). Given the observed restructuring of connectivity between specific DANs and KCs under different caloric conditions, we sought to understand how variation in food composition might affect associative odor learning. Appetitive associative olfactory learning, using sugar as a reward, is known to be influenced by the hunger/satiation state of the animals, with only starved flies capable of learning (Tempel et al. 1983). The impact of different food types on the starvation time required for animals to associate an odor with a sugar reward was analyzed. It was observed that the three types of food used—hypocaloric, isocaloric, and hypercaloric—clearly influenced the motivational hunger/satiation state of the flies, affecting their ability to engage in appetitive learning (Fig. 2A–C). Notably, in the absence of additional starvation, appetitive learning was absent (Fig. 2A). However, after 24 h of starvation, all animals, regardless of the caloric value of the food they were previously exposed to, exhibited significant appetitive olfactory learning (Fig. 2C). This finding indicates that all animals, irrespective of their prior diet, were healthy, capable of learning, and not experiencing severe malnutrition. Following a 6-h period of starvation, corresponding to an intermediate hunger/satiation state, flies previously exposed to hypocaloric food exhibited significantly higher learning scores in appetitive olfactory learning compared to those on hyper- or isocaloric diets (Fig. 2B). The effect of exposing the animals to low-caloric food for an extended period of time became visible when the animals were not extensively starved for 24 h or not starved at all. Although this result aligns with expectations, an intriguing discovery emerged in the context of aversive learning (Fig. 2D–F). Notably, in the absence of starvation, aversive learning was comparable across all food conditions (Fig. 2D), and this pattern persisted after 24 h of starvation (Fig. 2F). However, aversive learning was notably reduced after 6 h of starvation in animals that had been maintained on hypocaloric food (Fig. 2E). This surprising finding suggests a relationship between the duration of starvation, the caloric content of the food consumed before, and modulation of aversive learning. Naive repulsion from the odorants used for conditioning or avoidance of electric shocks as unconditioned stimuli was not affected by the feeding condition (Supplemental Fig. S1G,H). Apparently, the metabolic state of the animals, induced by keeping the animals on low-calorie food, had changed their ability to learn and/or retrieve memory in that aversive learning was reduced and appetitive learning enhanced, which became visible at intermediate satiation levels. This suggests that the balance between the two had shifted. We further explored that possibility by subjecting the animals to a conflicting situation in a counter-conditioning paradigm. Flies were first trained to associate an odor with a reward, and subsequently the same odor with a punishment (or vice versa). Then, it was tested whether they had formed (or retrieved) either an aversive or appetitive memory for the conditioned odor. The training was conducted after 6 h of starvation because the change in aversive and appetitive learning was observed at this time point. Interestingly, animals kept on hypocaloric food showed pronounced appetitive learning, but those kept on isocaloric or hypercaloric food behaved indifferently in that they were neither repelled nor attracted by the trained odor (Fig. 2G). After 6 h of starvation, aversive learning, or the retrieval of an aversive memory, was overridden by appetitive learning or memory retrieval. As a control, when the training procedure was exactly recapitulated in flies kept on hypocaloric food, but either aversive or appetitive training was omitted, a respective aversive or appetitive memory readout was observed (Fig. 2G, right). These data demonstrate that in a conflicting situation, it is the aversive memory that is either not formed or suppressed in favor of appetitive memory formation or retrieval.

Structural synaptic plasticity can be optogenetically mimicked by manipulating the cAMP level

Exposing the animals to hypocaloric food for 7 d caused structural plasticity in the physical connection between specific DANs and KCs and reduced aversive learning. We asked whether the two observed phenomena were actually linked or whether they represented correlations without a causal connection. First, we used functional GRASP in which one part (spGFP1-10) of the splitGFP is fused with the synaptic vesicle protein Synaptobrevin (MacPherson et al. 2015). Thereby, the splitGFP reconstitution represents a readout of functional synaptic connections and their actual activity in terms of vesicle release, rather than solely physical proximity. Exposing the animals to hypocaloric food led to a reduction in the intensity of the reconstituted splitGFP fluorescence, confirming that functional synaptic connections undergo plastic modifications in response to dietary conditions (Fig. 3A). To further elucidate the specific DANs labeled by MB188B-Gal4, we compared the reconstituted splitGFP fluorescence between KCs and MB188B-Gal4-labeled DANs with R58E02-Gal4, a driver line

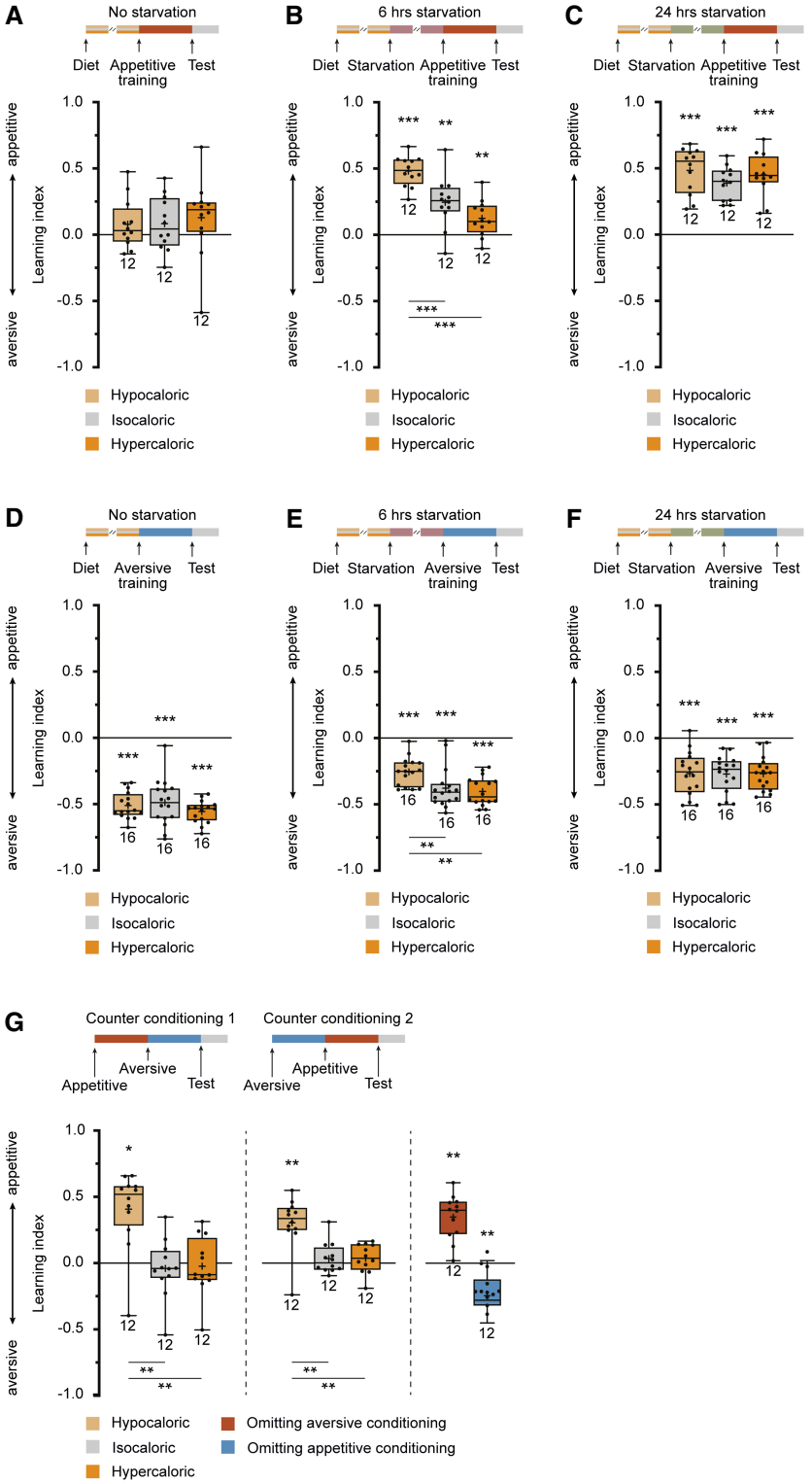

Figure 2. Calorie restriction affects appetitive and aversive associative olfactory learning. (*A*–*C*) Appetitive short-term memory after reward-mediated olfactory conditioning depends on the starvation/satiation state. Flies maintained on isocaloric food for 7 d without a period of starvation do not show significant appetitive learning (*A*, gray box). Learning indices increase when animals are starved for 6 h (*B*, gray box) or 24 h (*C*, gray box). Maintaining the animals on hypo- or hypercaloric food (light and dark orange boxes, respectively) does not affect learning, either positively or negatively, without starvation (*A*) or after 24 h of starvation (*C*). However, after 6 h of starvation, increased learning in flies maintained on hypocaloric food and decreased learning in flies maintained on hypercaloric food is detectable (*B*). (*D*–*F*) Aversive short-term memory after punishment-mediated olfactory conditioning likewise depends on the starvation/satiation state. Flies maintained on isocaloric food for 7 d without a period of starvation show significant aversive learning (*D*, gray box). Learning indices decrease when animals are starved for 6 h (*E*, gray box) or 24 h (*F*, gray box). Maintaining the animals on hypo- or hypercaloric food (light and dark orange boxes, respectively) does not affect learning, either positively or negatively, without starvation (*D*) or after 24 h of starvation (*F*). However, after 6 h of starvation, decreased learning in flies maintained on hypocaloric food becomes detectable (*E*). (*G*) In a counter-conditioning paradigm in which the same odor is first associated with a reward and, subsequently, with a punishment or vice versa, no learned preference or avoidance is observed in animals maintained on isocaloric or hypercaloric food. However, animals kept on hypocaloric food express an appetitive short-term memory, as indicated by positive learning indices. Control animals in which either aversive or appetitive conditioning was omitted (blue boxes) show either appetitive or aversive learning. Box plots indicate 25/75 percentiles, lines represent medians, whiskers represent min/max values, pluses represent means, dots represent individual data points, and numbers represent sample sizes. Statistically significant deviations from the baseline are indicated as asterisks above the boxes. Statistically significant differences between groups are indicated with asterisks and lines below boxes. For statistical tests, see Supplemental Tables S1–S4. (*) $P<0.05$, (**) $P<0.01$, (***) $P<0.001$.

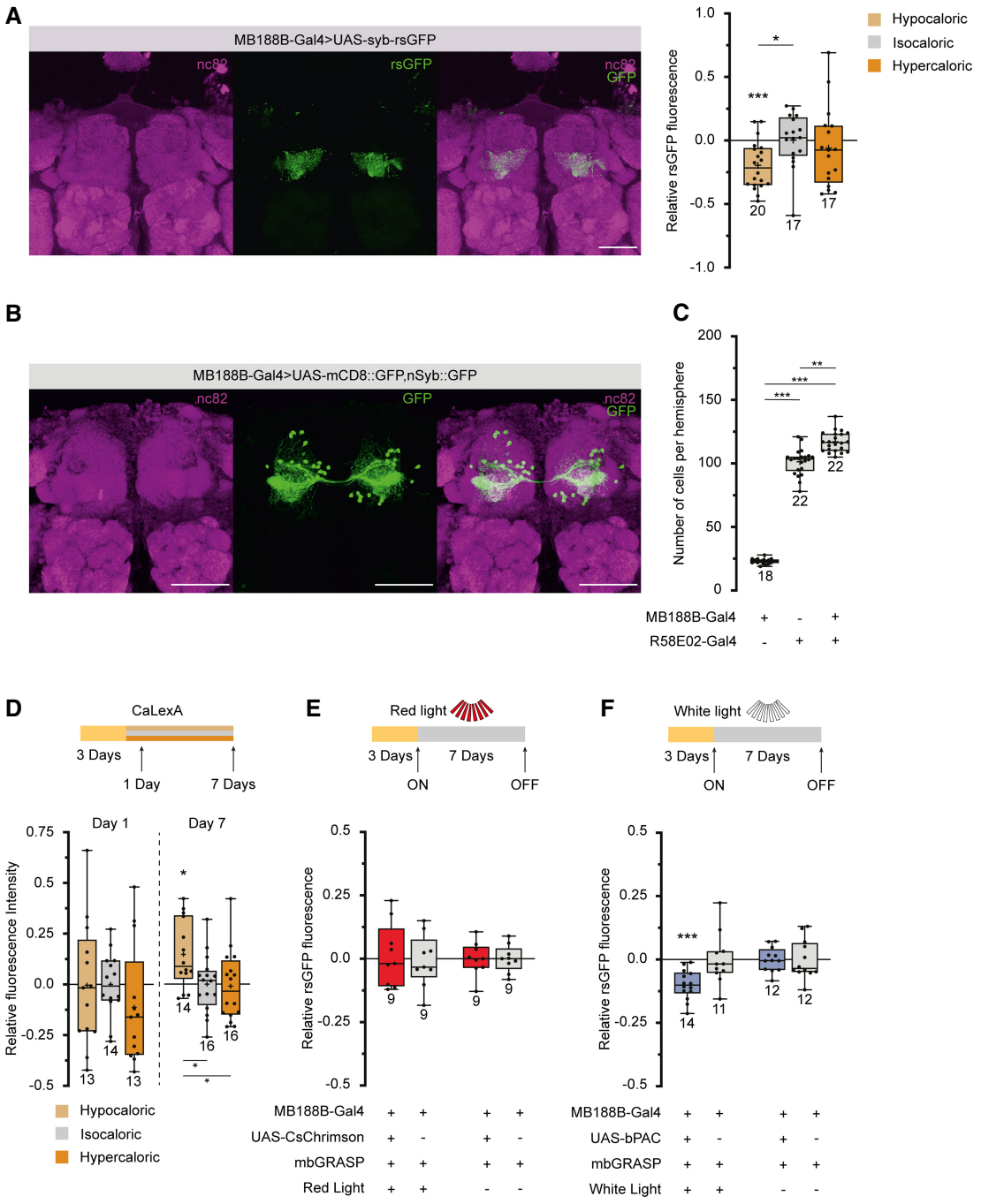

Figure 3. The decrease in connectivity between MB188B-Gal4-driven DANs and KCs can be optogenetically mimicked. (*A*, *Left*) *Z*-projection through a confocal microscopic stack visualizing the synaptic connectivity between MB188-Gal4-positive DANs and KCs using synaptobrevin-coupled GRASP. (Magenta) Immunohistochemical staining of the pan-neuronal presynaptic protein Bruchpilot (antibody nc82), (green) nSyb-GRASP fluorescence, and overlay of both. (*Right*) Quantification of relative rsGFP fluorescence intensity between populations of DANs and KCs. (*B*) Z-projection through a confocal microscopic stack visualizing the population of DANs labeled by MB188B-Gal4. (Magenta) Immunohistochemical staining of the pan-neuronal presynaptic protein Bruchpilot (antibody nc82), (green) expression of mCD8-GFP and nSyb-GFP under control of MB188B-Gal4, and overlay of both. (*C*) Quantification of somata labeled by either MB188B-Gal4, R58E02-Gal4, or both together. Sixty-eight percent of the cells targeted by MB188B-Gal4 are not part of those targeted by R58E02-Gal4. (*D*) Comparative quantification of sustained neural activity using the Ca^{2+}-dependent GFP expression system CaLexA in neurons labeled by MB188B-Gal4. Relative fluorescence intensity was significantly higher in flies maintained for 7 d on hypocaloric food, but not after only 1 d. (*E*) Optogenetic depolarization of MB188B-Gal4-positive neurons through pulsed red-light illumination using the photosensitive cation channel CsChrimson does not change splitGFP reconstitution between these DANs and KCs when compared with genetic control strains. (*F*) Optogenetic induction of cAMP synthesis in MB188B-Gal4-positive neurons through pulsed white-light illumination using the photosensitive adenylate cyclase bPAC decreases splitGFP reconstitution between these DANs and KCs when compared with the genetic control, thereby mimicking the effect of hypocaloric food. Scale bar, 50 µm. Box plots indicate 25/75 percentiles, lines represent medians, whiskers represent min/max values, pluses represent means, dots represent individual data points, and numbers represent sample sizes. Statistically significant deviations from the baseline are indicated as asterisks above the boxes. Statistically significant differences between groups are indicated with asterisks and lines below boxes. For statistical tests, see Supplemental Tables S1–S4. (*) $P<0.05$, (**) $P<0.01$, (***) $P<0.001$.

commonly used for analyzing all PAM-cluster DANs (Liu et al. 2012). The distinct regions of fluorescence indicated nonoverlapping populations of neurons (compare Figs. 1D,E and 3A). Counting somata revealed 23.0 ± 2.1 in MB188B-Gal4 ($n = 18$) and 101.3 ± 10.7 in R58E02-Gal4 per brain hemisphere ($n = 22$). The genetic combination of both Gal4 lines resulted in 117.0 ± 7.9 somata ($n = 22$) (Fig. 3B,C), demonstrating that ∼16 neurons, or ∼70% of MB188B-Gal4-positive neurons, are exclusively part of MB188B-Gal4 and not part of R58E02-Gal4.

Although previous studies suggested that very specific DANs innervating the γ3 compartment mediate reward learning when suppressed (Yamagata et al. 2016), our investigation using the respective driver line MB441B-Gal4 did not show an effect of caloric food conditions on contacts between KCs and these DANs (Supplemental Fig. S7A). This suggests that the observed plastic effect of decreased DAN–KC contacts is attributed to different subsets of DANs rather than those implicated in γ3 reward learning. To further investigate the impact of hypocaloric conditions on synaptic connectivity, we extended our analysis to KC connections with complementary MBONs innervating specific compartments. Notably, MBONs innervating the β′1 compartment also project to the γ3 compartment, akin to the DANs labeled by MB188B-Gal4. This suggests a functional compartmentalization across different KC types, specifically β′- and γ-lobe KCs. However, examining the reconstituted splitGFP fluorescence intensity between KCs and the respective MBONs using the split-Gal4 lines MB83C-Gal4 and MB110C-Gal4 (Scaplen et al. 2021) revealed that this connectivity was not influenced by the caloric value of food (Supplemental Fig. S7B,C). This suggests that, unlike the observed changes in dopaminergic mushroom body input neurons, the connections between KCs and MBONs were not affected by dietary conditions.

Moreover, we used a mosaic analysis of a repressible marker (MARCM) (Lee and Luo 1999) to examine the gross morphology of KCs of all three types (Supplemental Fig. S4A–C). This technique allowed us to label individual KCs with a red fluorescent marker protein against a background of all KCs marked in green fluorescence. The anatomical structures of KCs were then reconstructed in three dimensions and quantified based on various parameters, including the number of dendritic claws, lengths of axons and dendrites, number of axonal boutons, points of axonal bifurcations (nodes), and length of arborizations from primary axons, serving as measures of neuronal complexity. Exposing the animals to any of the three food compositions did not significantly modify any of these anatomical parameters (Supplemental Fig. S4A–C). This indicates that the synaptic changes quantified using the GRASP technique, which revealed alterations in dopaminergic mushroom body input neurons, were not accompanied by detectable anatomical changes in the individual KCs. In addition, we conducted a complete transcriptome analysis of fluorescence-activated cell sorted (FACS) KCs, and compared transcript levels between animals kept on isocaloric food with those kept on hypocaloric food. Out of 10,578 transcripts, only one single gene showed a significant up-regulation in animals kept on hypocaloric food, namely, the gene mei-P26 (Supplemental Fig. S5; Supplemental Table S6). The functions of this gene in developing germline cells are well-investigated; however, its role in the adult nervous system beyond neuronal differentiation remains less understood (Neumüller et al. 2008), and an analysis of the function of this gene in the mushroom body is beyond the scope of this study. Nevertheless, we notice that significant differences in transcript levels between the two feeding conditions in KCs are surprisingly scant, indicating that the modifications might take place in DANs. In sum, we conclude that the changes in synaptic connectivity most likely arise from modifications within DANs and their reciprocal synapses with KCs. However, we acknowledge that subtle changes in KCs, which may be below the spatial resolution of our microscopic analysis, such as alterations at specific postsynaptic densities or presynaptic active zones, cannot be excluded.

To test for a potential causal connection between behavioral alterations induced by caloric restriction and the observed synaptic plasticity, we evaluated whether the decrease in synaptic connectivity could be artificially mimicked. MB188B-Gal4-positive DANs showed a slightly higher neuronal activity when the animals were fed hypocaloric food for 7 d, as revealed using CaLexA, a GFP-based reporter whose transcription is controlled by the neuronal Ca^{2+} level as a general correlate of neuronal activity (Fig. 3D; Masuyama et al. 2012). However, when the light-sensitive cation channel CsChrimson (Klapoetke et al. 2014) was expressed under control of MB188B-Gal4 and pulsed, red-light illumination of the animals was applied over a period of 7 d, no alteration of the splitGFP reconstitution was observed (Fig. 3E). This indicates that depolarization per se does not cause any decrease in connectivity, in contrast to what was observed under prolonged hypocaloric conditions. We then asked whether modulatory second-messenger pathways, such as the cAMP-dependent signaling cascade, might induce the decrease in synaptic connectivity. To test this, the light-inducible adenylate cyclase bPAC (Stierl et al. 2011) was expressed in MB188B-positive DANs, and the animals were illuminated with pulses of white light for 7 d. Indeed, optogenetically raising the cAMP level was sufficient to induce a decrease in the connectivity between MB188B-DANs and KCs, similar to the effect observed after keeping the animals on hypocaloric food (Fig. 3F). On the one hand, this finding provided an experimental approach to artificially mimic synaptic plasticity in order to test which behavioral alteration this might cause. On the other hand, it raised the question of which natural modulator could potentially affect cAMP signaling in these DANs.

Allatostatin A receptors, but not SIFamide receptors, are required for synaptic plasticity

Allatostatin A (AstA), a neuropeptide signaling satiety (Hergarden et al. 2012), has already been reported to influence DANs innervating the mushroom body (Yamagata et al. 2016). In accordance with this report, our immunohistochemical stainings indeed indicated a close proximity of AstA immunoreactivity and MB188B-Gal4-positive DANs (Fig. 4A). To test whether such AstA-mediated input to MB188B-Gal4-DANs is involved in inducing calorie-dependent synaptic modifications, an RNAi construct against the AstA1 receptor was expressed in MB188B-Gal4-positive DANs. Expression of this RNAi construct under the control of MB188B-Gal4 caused an increase in sucrose uptake (Fig. 4B). RNAi-mediated down-regulation of the AstA1 receptor in DANs prevented the synaptic plasticity induced by keeping the animals on hypocaloric food as judged by the unchanged reconstituted splitGFP fluorescence between test and control group (Fig. 4C). Additionally, we tested for a potential involvement of SIFamide, which represents a further neuropeptide involved in signaling states of hunger, and SIFamidergic neurons send projections to the mushroom body (Martelli et al. 2017). Anti-SIFamide immunoreactivity also indicates a potential proximity between SIFamide and MB188B-Gal4-positive DANs (Fig. 4D). Likewise, RNAi-mediated down-regulation of the sole SIFamide receptor that exists in flies (Park et al. 2014) caused a slight increase in sucrose uptake, which was statistically different from only one heterozygous parental control strain (Fig. 4E). However, expression of this RNAi did not prevent the decrease in synaptic connections between MB188-DANs and KCs because of hypocaloric conditions (Fig. 4F). Together, these data indicate that the satiety-signaling

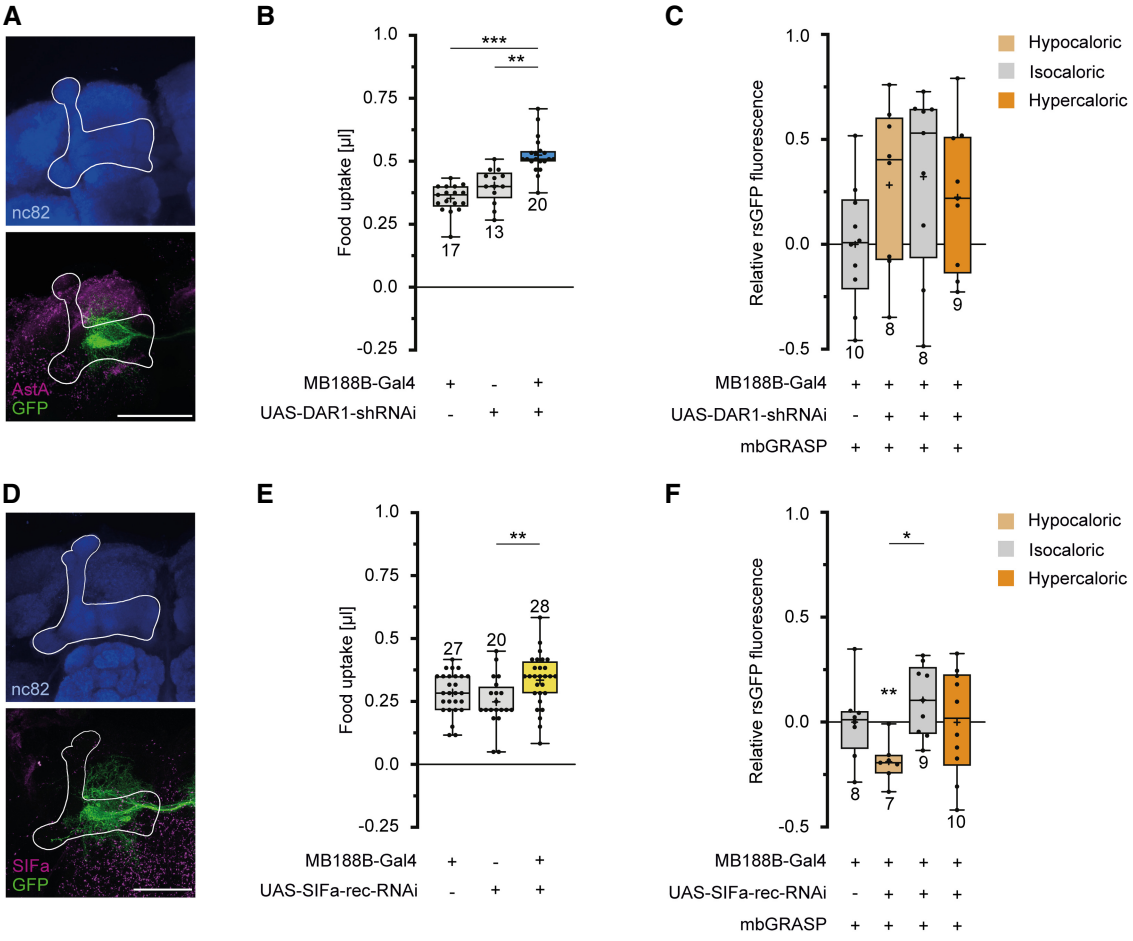

Figure 4. An AstA receptor, but not the SIFamide receptor, is required for a decrease in connectivity between MB188B-Gal4-targeted DANs and KCs induced by low-caloric food. (*A*) *Z*-projection through a confocal microscopic stack visualizing AstA immunoreactivity (magenta) and GFP expression in MB188B-Gal4-targeted DANs (green) innervating the mushroom body (white outline). The mushroom body is localized through immunostaining against Bruchpilot using the nc82 antibody (blue). (*B*) Quantification of food uptake using the capillary feeding (CAFE) assay in flies with RNAi-mediated knockdown of the AstA receptor 1 (DAR1) in MB188B-Gal4-targeted DANs, compared with genetic control strains. (*C*) Quantification of relative rsGFP fluorescence between MB188B-Gal4-targeted DANs and KCs in flies with RNAi-mediated knockdown of DAR1 in MB188B-Gal4-targeted DANs and in different feeding conditions. Hypercaloric food does not significantly alter the connectivity between these DANs and KCs when DAR1 is down-regulated. (*D*) Z-projection through a confocal microscopic stack visualizing SIFamide immunoreactivity (magenta) and GFP expression in MB188B-Gal4-targeted DANs (green) innervating the mushroom body (white outline). The mushroom body is localized through immunostaining against Bruchpilot using the nc82 antibody (blue). (*E*) Quantification of relative food uptake using the CAFE assay in flies with RNAi-mediated knockdown of the SIFamide receptor (SIFa-rec) in MB188B-Gal4-targeted DANs, compared with genetic control strains. (*F*) Quantification of relative rsGFP fluorescence intensity between MB188B-Gal4-targeted DANs and KCs in flies with RNAi-mediated knockdown of SIFa-rec in MB188B-Gal4-targeted DANs and in different feeding conditions. The decrease in the connectivity between these DANs and KCs when flies are maintained on hypocaloric food remains when SIFa-rec is down-regulated. Scale bar, 50 µm. Box plots indicate 25/75 percentiles, lines represent medians, whiskers represent min/max values, pluses represent means, dots represent individual data points, and numbers represent sample sizes. Statistically significant deviations from the baseline are indicated as asterisks above the boxes. Statistically significant differences between groups are indicated with asterisks and lines above boxes. For statistical tests, see Supplemental Tables S1–S4. (*) $P<0.05$, (**) $P<0.01$, (***) $P<0.001$.

neuropeptide AstA influences MB188B-DANs and their synaptic connections with KCs.

Structural synaptic plasticity between specific dopaminergic neurons and Kenyon cells modifies olfactory associative learning

The current data imply that caloric restriction induces a cAMP-dependent modulation of MB188B-Gal4-positive DANs, resulting from a decreased input from ASTA-releasing neurons. This, in turn, leads to a reduction in synaptic connectivity between these DANs and KCs. To further explore whether the observed decrease in synaptic connectivity affects olfactory learning in a manner similar to the exposure of flies to hypocaloric food, we focused on the γ3 compartment of KCs to assess responses to punishing electric shocks.

Given that dopamine release on KCs acts, at least partially, on type 1 dopamine receptors coupled to $G_{\alpha/s}$ proteins that activate adenylate cyclases, we used the fluorescent cAMP sensor G-Flamp1 (Wang et al. 2022). This sensor was expressed in γ-lobe KCs, and in vivo two-photon microscopy was used to monitor the effects of a series of electric shocks, as typically presented in aversive olfactory conditioning experiments (Fig. 5A; Supplemental Fig. S6). In the γ2 compartment, electric shocks induce local increases in cAMP levels in KCs that reflect the time course of the shocks (Supplemental Fig. S6A), consistent with their input from punishment-mediating PPL1-cluster DANs (Riemensperger et al.

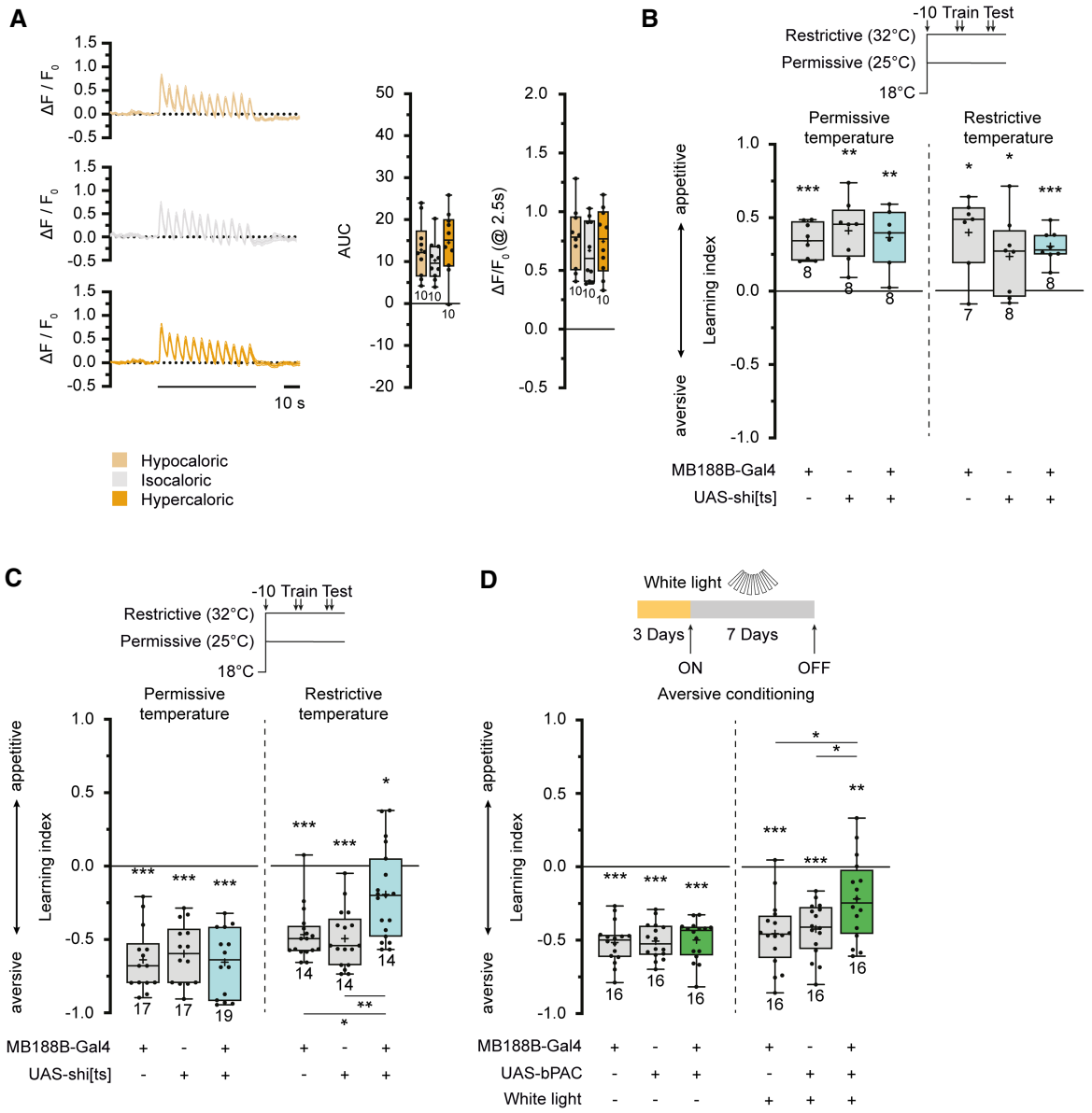

Figure 5. MB188B-Gal4-targeted DANs are required for aversive olfactory learning. (*A*) Optical imaging of cAMP dynamics in the γ3 compartment of the mushroom body in response to a series of punishing electric shocks in animals maintained for 7 d on food of different caloric values. (*Left*) Relative changes in fluorescence intensity of the cAMP sensor Flamp1 in response to 12 consecutive electric shocks. (*Middle*) Integral of relative changes in fluorescence intensity (area under curve, AUC). (*Right*) Maximum amplitude of relative changes in fluorescence intensity. (*B*) Blocking synaptic transmission in MB188B-Gal4-targeted DANs through temperature-sensitive shibire expression does not affect appetitive, reward-based learning. (*C*) Blocking synaptic transmission in MB188B-Gal4-targeted DANs through temperature-sensitive shibire expression impairs aversive, punishment-based learning. Flies have been shifted from 18°C to the restrictive (32°C) or the permissive temperature (25°C) 10 min before training. (*D*) Stimulating cAMP synthesis optogenetically using bPAC expression in MB188B-Gal4-targeted DANs for 7 d before conditioning impairs aversive, punishment-based learning. Line diagrams indicate means ± SEM. Box plots indicate 25/75 percentiles, lines represent medians, whiskers represent min/max values, pluses represent means, dots represent individual data points and numbers represent sample sizes. Statistically significant deviations from the baseline are indicated as asterisks above the boxes. Statistically significant differences between groups are indicated with asterisks and lines above or below boxes. For statistical tests, see Supplemental Tables S1–S4. (*) $P<0.05$, (**) $P<0.01$, (***) $P<0.001$.

2005), and the γ3 compartment exhibited equivalent cAMP transients evoked by electric shocks (Fig. 5A). However, the γ4 and γ5 compartments did not show comparable responses (Supplemental Fig. S6B,C). Surprisingly, the quantitative change in fluorescence of the cAMP sensor did not differ between the three feeding conditions (Fig. 5A). This leads us to conclude that either the decrease in connectivity between MB188B-Gal4-positive DANs and KCs is not robust enough to be detectable using the fluorescent cAMP imaging approach, or there might be additional neurons not covered by MB188B-Gal4 that convey electric shock signals to the γ3 compartment. However, the finding that the γ3 compartment is actually responsive to electric shocks prompted us to test whether transmitter release from MB188B-Gal4-positive DANs is required for associative learning. The dominant-negative temperature-sensitive dynamin variant shibire^{ts} (Kitamoto 2001) was used to block synaptic transmission from MB188B-Gal4-

positive DANs during olfactory conditioning and memory retrieval. Appetitive associative learning was unaffected at both the permissive and restrictive temperature (Fig. 5B), demonstrating that synaptic output from these DANs is not required for olfactory reward learning and short-term memory formation. In contrast, aversive associative learning using electric shocks as unconditioned stimuli was severely impaired at the restrictive temperature (Fig. 5C), demonstrating that, unexpectedly, output from these PAM-cluster DANs was required for aversive learning and/or short-term memory formation. Optogenetically depolarizing or hyperpolarizing MB188B-Gal4-DANs using either the cation channel CsChrimson (Klapoetke et al. 2014) or the anion channel *Gt*ACR1 (Govorunova et al. 2015) did not affect food uptake (Supplemental Fig. S8A,B).

Because exposing the animals to hypocaloric food caused a reduction in the connections between MB188-Gal4-positive DANs and KCs, and this effect could be mimicked using optogenetic manipulation of cAMP levels, we asked whether such an optogenetic manipulation would, in turn, affect aversive learning. We found that, indeed, exposing flies that expressed bPAC under control of MB188B-Gal4 to pulsed white light for a period of 7 d caused a significant decrease in aversive olfactory learning and/or short-term memory formation (Fig. 5D). These data close the full circle: Caloric restriction induces structural synaptic plasticity in specific DAN–KC connections that are causative for a decrease in aversive odor learning or the retrieval thereof.

Discussion

The brain's capacity to reorganize itself in response to experiences, stimuli, and internal states is a fundamental aspect of its functioning, crucial for maintaining cognitive flexibility throughout life. This adaptive plasticity of brain networks in processing information is most commonly understood within the context of alterations in synaptic transmission. However, it also includes structural plasticity, which involves changes in the number and/or structure of neurons or synapses, representing a widespread process to modify and adjust network function. Structural plasticity involves the dynamic processes of synapse formation, stabilization, and elimination (Holtmaat and Svoboda 2009). These modifications can be observed at the level of synapses or synaptic structures, such as dendritic spines or axonal boutons. Furthermore, structural plasticity operates at subsynaptic, molecular levels, involving the remodeling of presynaptic active zone proteins or postsynaptic densities. It can even manifest at the macrostructural level, leading to volume changes in entire brain regions, such as specific parts of the cortex (for review, see Lövdén et al. 2013). The multifaceted nature of structural plasticity allows the brain to continuously adapt its architecture in response to various stimuli, contributing to the dynamic nature of neural networks and cognitive processes. The mushroom body of the insect is no exception in its ability for structural rewiring. In *Drosophila melanogaster*, the size of the presynaptic boutons of projection neurons in the mushroom body calyx is plastic and dependent on neuronal activity (Kremer et al. 2010; Pech et al. 2015), which provides evidence for activity-dependent structural reorganization of a circuit. Moreover, the formation of an appetitive associative long-term memory for a particular odor is accompanied by a structural change in the presynaptic, calycal boutons (Baltruschat et al. 2021). Likewise, in honeybees, volumetric changes in mushroom body structures, particularly in the calyx, correlate with experience and age (Withers et al. 1993; Durst et al. 1994; Maleszka et al. 2009; Hourcade et al. 2010; Groh et al. 2012). These studies provide evidence that in the insect mushroom body, sustained or blocked sensory input, as well as experience such as associative learning of sensory cues, can structurally modify circuit structures implemented to encode sensory representations. Our finding that DANs, which contribute to reinforcing valence signaling in an insect brain, also undergo plastic modifications adds a new level of complexity.

Current models of the mechanisms and neuronal circuits of olfactory associative learning in the insect brain often highlight the dichotomy between rewarding and punishing signals, orchestrating either aversive or appetitive learning. Initially, this dichotomy seemed to be a product of the artificial laboratory setup, rooted in the conventional T-maze and binary choice behavior paradigm (Tempel et al. 1983; Tully and Quinn 1985). However, the clear division between positive and negative valences is not solely an experimental artifact. The γ-lobe of the mushroom body emerges as a pivotal player in associative learning and short-term memory retrieval postlearning (Zars et al. 2000; Qin et al. 2012). Synaptic depression in the γ1 and γ2 compartments is implicated in aversive learning, whereas synaptic depression in the γ4 and γ5 compartments is associated with appetitive learning (Hige et al. 2015; Hancock et al. 2022). This dichotomy is seemingly mirrored in the punishment-signaling DANs of the PPL1 cluster, which innervate γ1 and γ2, and the reward-mediated DANs of the PAM cluster, which innervate γ3–γ5. However, optical measurements of Ca^{2+} transient in KCs reveal that only the γ4 and γ5 compartments (not γ3) respond to rewarding stimuli (Cohn et al. 2015), contrary to the prevailing view. Conversely, our cAMP transient measurements show that the γ2 and γ3 compartments respond to punishing stimuli, in accordance with Wang et al. (2022). Therefore, this study adds a more nuanced aspect to the established categorization of DANs into punishing PPL1 and rewarding PAM clusters. One might perhaps hypothesize a role for the γ3 compartment in balancing appetitive and aversive learning, given its central position along the γ-lobe. In fact, it has been shown that MB188B-Gal4-positive DANs modulate polyamine odor attraction bidirectionally dependent on the mating state (Boehm et al. 2022), which suggests multiple roles of these DANs in different behavioral contexts and corroborates their function in balancing antagonistic behaviors. Moreover, the PAM-cluster DANs innervating the γ3 compartment do not seem to form a functionally uniform population, introducing complexity to the traditional model. Notably, subpopulations of DANs innervating the γ3 compartment targeted by other Gal4 lines than those studied here influence appetitive learning in that their suppression mediates reward (Yamagata et al. 2016). However, our finding that AstA signaling affects these DANs is in accordance with the report of Yamagata et al. (2016) that describes an inhibition of γ3-innervating DANs by AstA. If AstA signals satiety, as reported by Hergarden et al. (2012), it is reasonable to assume that hypocaloric conditions might suppress AstA release. Because the AstA receptor has been reported to be $G\alpha_{i/0}$-coupled (Larsen et al. 2001), satiety signaled through AstA-releasing neurons would potentially inhibit adenylate cyclases and cAMP synthesis. With the same logic, hypocaloric conditions might in turn lead to elevated cAMP levels that are causative for the decline in synaptic connections with KCs. The RNAi-mediated down-regulation of the AstA1 receptor would then disrupt the neurons' capacity of modulation by different caloric values. Of course, we do not exclude the possibility that hunger-signaling peptides might also be involved, which might act as counter players of AstA that induce cAMP synthesis.

An intriguing observation is that MB188B-Gal4-positive DANs innervate both the γ3 and β′1 compartments. This aligns with some corresponding MBONs that also innervate the equivalent compartments, suggesting that compartments across multiple KC types (γ-lobe and β′ KCs) constitute functional units. A clear functional subdivision of the different KC types in balancing appetitive and aversive learning is, therefore, not to be expected.

We ascribe the observed structural plasticity to alterations within the investigated DANs. Nevertheless, it is imperative to acknowledge the possibility that KCs, which maintain synaptic connections with the aforementioned DANs, might also undergo modifications within their respective compartments. Given the existence of reciprocal synapses (Cervantes-Sandoval et al. 2017), the intricate nature of the synaptic modifications becomes apparent and adds a layer of complexity in discerning whether pre- and/or postsynaptic elements in DANs and potentially KCs are subject to modification. The precise nature of these modifications remains elusive, and it is unclear whether they occur predominantly in pre- or postsynaptic regions of DANs and if they potentially extend to KCs. Furthermore, a comprehensive understanding of the physiological impact of the observed structural plasticity on synaptic transmission remains elusive. Recent reports indicate that increases in cAMP levels in addition with KC activation lead to synaptic depression, with temporal differences across KC compartments (Yamada et al. 2024), as is the case in aversive associative learning (Hancock et al. 2022). The decrease in synaptic connectivity might perhaps influence the generation of learning-induced synaptic depression. However, it remains imperative to conduct further studies at the synaptic level to elucidate the effects of structural plasticity on synaptic transmission.

Materials and Methods

Fly husbandry

All fly stocks used in this study are listed in Supplemental Table S5. All flies were raised until eclosion on standard cornmeal-based medium under a 12-h light–dark cycle, and at 25°C temperature and 60% humidity unless otherwise indicated. The *Drosophila* food compositions were as follows:

Standard cornmeal medium: 80 g/L cornmeal, 10.25 g/L agar, 10 g/L soy flour, 18 g/L yeast, 22 g/L sugar beet syrup, 80 g/L malt, 6.3 mL/L propionic acid, 1.5 g/L nipagin, 7 mL/L ethanol.
Hypocaloric food: 80 g/L cornmeal, 5 g/L agar, 20 g/L sucrose, 2.5 g/L yeast, 6.3 mL/L propionic acid (36 kcal/100 g).
Isocaloric food: 80 g/L cornmeal, 5 g/L agar, 50 g/L sucrose, 20 g/L yeast, 6.3 mL/L propionic acid (52 kcal/100 g).
Hypercaloric food: 80 g/L cornmeal, 5 g/L agar, 150 g/L sucrose, 20 g/L yeast, 10 g/L pork lard, 6.3 mL/L propionic acid (100 kcal/100 g).

To starve flies, the animals were placed in vials containing a wetted paper tissue.

Quantification of splitGFP reconstitution

Flies were anesthetized on ice for at least 10 min and the brains of 5- to 7-d-old female flies were removed from the head capsule. The tracheae were carefully removed and the brains were placed in cold Ringer's solution containing 5 mM HEPES (pH = 7.3), 130 mM NaCl, 5 mM KCl, 2 mM $MgCl_2$, 2 mM $CaCl_2$, and 36 mM sucrose (Estes et al. 1996). Subsequently, the brains were transferred to 4% paraformaldehyde solution (pH = 7.4) and incubated for 30 min at room temperature followed by three washing steps of at least 15 min each with 0.6% Triton X-100 in phosphate-buffered saline (PBST) and mounted in Vectashield (Vector Laboratories). Image stacks were obtained using a Leica TC SP8 confocal microscope and a 20×/0.7 water/glycerol immersion objective at 1-µm steps in the *z*-axis. The same settings (resolution, laser power, zoom factor) were used for every repetition of the same experiment. Fluorescence intensity in distinct regions of interest was quantified using Fiji (Schindelin et al. 2012). The brains were not subjected to any staining and raw fluorescence was quantified.

Immunohistochemistry

Five- to seven-day-old female flies were used, with the exception that 10-d-old female flies were used for experiments that involved sustained feeding of calorie-modified food or optogenetic manipulation. Flies were anesthetized for at least 10 min on ice, and the brains were dissected in ice-cold Ringer's solution. Subsequently, the brains were transferred to 4% paraformaldehyde solution and incubated for 30 min at room temperature followed by three washing steps of at least 15 min each in PBST. Blocking was performed in 2% bovine serum albumin dissolved in PBST overnight at 4°C. After blocking, the brains were incubated in primary antibodies dissolved in blocking solution for at least 6 h at room temperature, followed by three washing steps of at least 15 min each in PBST, and subsequent incubation with secondary antibodies dissolved in blocking solution overnight at 4°C. The samples were washed three times for at least 15 min in PBST and mounted in Vectashield (Vector Laboratories) before microscopy. Image stacks were obtained using a Leica TC SP8 confocal microscope and a 20×/0.7 water/glycerol immersion objective at 1-µm steps in the *z*-axis. The antibodies used in this study are listed in Supplemental Table S6.

Illumination for optogenetic experiments

Flies were stimulated using a custom-built chamber (optostimulator) that had the walls covered with LED panels. The vials containing the flies were placed in the chamber for the duration of the experiments. The duration and frequency of the light stimulation pulses were controllable. A chamber with white LEDs (160 lm/W, luminous flux 1.885 lm) was used for bPAC, and one with red LEDs (615–650 nm) was used for CsChrimson. Thirty-second light pulses at 10% of the maximum light intensity were applied every minute during the daytime of the 12 h:12 h light–dark cycle. No light stimulation was applied at night. The flies expressing CsChrimson or GtACRI were kept on food containing 250 mM all-*trans*-retinal throughout. Before light stimulation, flies carrying CsChrimson, GtACRI, or bPAC were reared in constant darkness.

Proboscis extension response

Flies were starved for 24 h at 25°C in a vial in which a wetted tissue paper was placed on the bottom. The starved flies were briefly anesthetized on ice and tethered into a 1-mL pipette tip using a three-component dental glue. Each fly was briefly touched on the labellum with a 2 M sucrose solution-soaked cotton swab. This procedure was repeated five times per fly, and proboscis extension incidents were scored as a percentage of proboscis extension responses (PERs).

Associative learning

Olfactory associative learning experiments were performed as described by Tempel et al. (1983) and Tully and Quinn (1985). A custom-built T-maze machine, described in Schwaerzel et al. (2002), was used to test four experimental groups of flies simultaneously. A mixed population of 50–70 male and female flies was trained by presenting an odor as conditioned stimulus (CS+) together with a rewarding or punishing unconditioned stimulus (US) for 1 min. 3-Octanol and 4-methylcyclohexanol were used as odorants at a 1:36 dilution. After a 1-min break, a second odor was presented as the CS– for another minute. A Whatman paper soaked with 2 M sucrose that covered the inside of a tube was used as the rewarding US; a series of 12 electric shocks of 90 V (1.25-sec shocks presented at 5-sec intervals) was administered as the punishing stimulus, via a tube covered on the inside with an electrifiable grid. One minute after training, the flies were transferred to the T-maze part of the apparatus. Flies were presented with CS+ and CS– odors simultaneously from different arms of the maze for 2 min with a constant airflow (167 mL/min). The number of flies in each arm was counted and a performance index was calculated as the number of flies in the CS+ arm minus the number of flies in the CS– arm divided by the total number of flies tested. Learning indices were calculated by averaging the two

performance indices of two reciprocal trainings in which the odorants used as CS+ or CS– were exchanged. During the starvation before the training procedure, the flies were placed in vials that contained filter paper soaked with tap water for either 6 or 24 h at 25°C. In experiments in which synaptic transmission was blocked using temperature-sensitive shibire expression (Kitamoto 2001), the permissive temperature was controlled and kept at 25°C. In the restrictive condition, the temperature of the chamber was increased to 32°C before learning experiments, and the flies were exposed to the restrictive temperature for at least 10 min before testing.

Electric shock avoidance and odor avoidance

Shock avoidance was tested using the same machine used for associative olfactory learning. The flies were placed in the middle compartment of the T-maze. One arm was equipped with either a tube covered with an electrifiable grid delivering 12 electric shocks (90 V, 1.25 sec in duration each) or with a tube equipped with an odorant container; the opposite arm contained only the solvent mineral oil with no odorant. The flies were allowed to roam freely in the apparatus for 2 min. A preference index was calculated as the number of flies in the arm containing the odor or in the electrified tube, respectively, minus the number of flies in the opposite arm divided by the total number of flies.

Capillary feeding assay

The CAFE assay was conducted as described by Ja et al. (2007). Individual female flies were starved for 24 h at 25°C in single vials containing a filter paper soaked with tap water. Following starvation, 1 M sucrose solution, unless stated otherwise, colored with red food dye was provided to each vial via a capillary tube by piercing the sponge vial plug. The sucrose level before and after 24 h of the assay was marked and a millimetric measurement of the solution level was converted into volume. Empty vials with capillaries were used to measure the amount of sucrose solution loss due to evaporation and this value was subtracted from each value.

FlyPad feeding assay

CantonS flies used in the FlyPad experiments were reared and maintained on standard cornmeal food, with the above-described composition, in incubators at 25°C, with 60% humidity, and under a 12 h:12 h light–dark cycle. After hatching, 3-d-old female flies were collected and transferred to hypo-, iso-, or hypercaloric food for 7 d. Five microliters of 1 M sucrose solution containing 1% low gelling temperature agarose were placed in wells of the FlyPad containing electrodes to detect the capacitance change when the flies physically interacted with the food. The flies were transferred to the FlyPad individually using a pump. The experiments were performed in a climate chamber at 25°C, at 60% humidity. Each FlyPad recording session lasted 60 min, during which time the flies could interact with the food ad libitum. For optogenetic manipulation experiments in the FlyPad, flies were reared and maintained on standard cornmeal food, as described previously, supplemented with all-*trans*-retinal at 0.2 mM concentration, in incubators at 25°C, under a 12 h:12 h light–dark cycle and 60% humidity. During the experiment, carried out in the dark, the flies were exposed to red (2-V) or green (5-V) light that was automatically activated once the fly started to sip 1 M sucrose food, as described above. Data were acquired using scripts (https://github.com/ribeiro-lab/optoPAD-software) based on Bonsai, an open-source program. Analysis was conducted using a MATLAB code.

Olfactory exploration assay

The discovery rate of individual flies was quantified using high-speed videography. Flies were situated in a circular arena with a diameter of 90 mm, which was sealed using an antiglare Perspex plate. A gap of 2 mm between the pane and the medium enabled the flies to move while restricting their ability to fly. To ensure that illumination was controlled, the camera and arena were placed in an enclosure that provided complete isolation from external light sources. High-speed videography was conducted from an overhead perspective at a frame rate of 50 Hz. For illumination, infrared LEDs (Pollin Electronic GmbH 53109) were placed beneath the arena. Data capture was executed using TroublePix software from NorPix Inc., and facilitated through a MotionTraveller 500 camera (Imaging Solutions GmbH). Each fruit fly's trajectory, consisting of position and orientation in each camera frame, was meticulously tracked using LACE, an automatic animal tracking system (Garg et al. 2022). Locomotion speed was determined by calculating the difference vector between the centers of mass in two consecutive frames. Furthermore, rotations in the yaw orientation were measured as the relative change in the orientation of the caudal–cranial axis across succeeding frames. LACE records the outline and surface area of the fly at each frame, aggregating these data to create a single polygon representing all of the locations the fly has visited during the observation period. Under conditions devoid of light, the surface area the animal has traversed becomes the area explored. Dividing the traversed area by the observation duration renders the exploration rate, quantified as square millimeters per second.

Quantification of survival rates

For every experiment, 10 flies (five males and five females) raised on standard food were collected immediately after eclosion and placed on different food conditions. The flies were transferred to a fresh food vial every third or fourth day. The dead flies left in the vial were counted during these transfers. Survival rates were calculated as the percentage of surviving flies for each time point. Each experiment was repeated five to six times for each condition. Male and female flies were pooled because the survival was not dependent on gender.

In vivo two-photon cAMP imaging

Female flies were briefly anesthetized on ice and mounted with clear sticky tape in a custom-built chamber that allowed for the delivery of electric shocks ventral to the fly's body. The fly head was fixed using light-cured composite resin and covered in Ringer's solution containing 5 mM HEPES (pH = 7.3), 130 mM NaCl, 5 mM KCl, 2 mM $MgCl_2$, 2 mM $CaCl_2$, and 36 mM sucrose (Estes et al. 1996). The head capsule was opened and the brain was exposed. In vivo imaging was performed using a two-photon laser-scanning microscope LSM 7MP (Zeiss) and Zeiss Zen software (2011 SP4 black edition), equipped with a W Plan-Apochromat 20×/1.0 water immersion objective (Zeiss). An excitation wavelength of 920 nm with a Ti:sapphire laser (Coherent Chameleon) was used in combination with a 500- to 550-nm BP filter. Images were captured at a pixel size of 0.42 µm and a frame rate of 4 Hz. Electric shock pulses were controlled via a custom-built controlling device. Flies were subjected to 12 90-V shocks spaced over 60 sec, each lasting 1.2 sec. The γ2–γ5 compartments of the mushroom body were observed simultaneously for each fly, with 10 individual flies for each food condition. Images were processed using Fiji (Schindelin et al. 2012). Raw image sequences were motion-corrected using the TurboReg plug-in (Thévenaz et al. 1998). Mean fluorescence intensities F over time were calculated from regions of interest within the γ-lobe compartments. The baseline fluorescence, F_0, was determined as the mean value of the 5-sec time frame before the onset of the first shock. The integral area under curve (AUC) was calculated for the 60-sec period of electric shocks and the maximum $\Delta F/F_0$ was determined as the value 2.5 sec after the onset of the first shock.

MARCM-dependent single Kenyon cell analysis

To visualize single-cell clones using MARCM (Lee and Luo 1999), the following genotype was generated:

hsFlp, −*Gal*80, w^-, *FRT*19*A*/γ, w^-, *FRT*19*A*;
*mb*247 − *GCaMP*3.0/+; 20*x UAS*:6 *x mCherry*/+;
OK107−Gal4/+

To induce heat-shock promoter–dependent flippase (flp) expression (Golic 1991), the food vials containing the respective larvae were placed in a water bath heated to 37°C using a custom-built device to keep the vials below the surface. The heat shock was applied for 2–4 h, interrupted by several breaks of 15–30 min at room temperature to avoid overheating of the larvae. Depending on the type of KC clone that was to be induced by MARCM, the larvae were heat-shocked at different time points after hatching. Heat shocks were applied for labeling of the respective KC types following Lee and Luo (1999). Brains were dissected, and subjected to immunohistochemical staining and confocal laser scan microscopy as described above. KC morphologies were reconstructed manually using the software Neurolucida. The reconstruction was performed using the simple click-tracing function. Only the skeletons of KCs were traced, ignoring different volumes along the neurites. Using the background marker expression (MB247-GCaMP3.0) for orientation, mushroom body substructures were identified. Accordingly, different parts of single KCs were assigned to the calyx, the peduncle, and the lobes, which in turn were further subdivided into different compartments, as described in Aso et al. (2014a) and Tanaka et al. (2008). Arborization lengths and the number of nodes were measured in the different cell subdivisions. Moreover, the dendritic claws within the calyx were marked and quantified. In cases where the image quality of a KC was considered to be very good, all bouton-like varicosities along the KC axons in the lobes were quantified. The primary node of a γ-lobe KC was defined within one of the five γ-lobe compartments according to the following criteria, taking into account the complexity of the arborizations: The node at a bifurcation was considered to be a primary node if, after bifurcation, both branches crossed at least two compartment borders. In the case of a bifurcation in the γ4 compartment, the node at the bifurcation was considered to be a primary node if both branches crossed the border to the γ5 compartment and were of the same magnitude. In the case of the analysis of α/β in the context of different caloric food conditions, only α/β surface neurons were reconstructed in order to avoid bias in the data set.

Kenyon cell sorting and RNA sequencing

Flies expressing DsRed in KCs under direct control of the promoter mb247 (Riemensperger et al. 2005) were transferred 3 d after hatching from standard food to either hypo- or isocaloric food, and were maintained there for 7 d. KCs were sorted similarly to Alyagor et al. (2018). In short, brains from 70 flies per replicate and food condition were dissected in ice-cold Ringer's solution. The collected samples were incubated in a collagenase/dispase mix (Roche 10269638001) for 30 min at 29°C. The samples were mixed every 5 min for efficient dissociation by flipping the tubes. Then, the samples were washed in dissociation solution (Sigma-Aldrich C1544) and transferred through a 35-µm mesh (Falcon) to eliminate remaining cell clusters and debris. Between 8000 and 15,000 DsRed-positive cells were sorted with low pressure through a flow cytometer (BD FACSAria Fusion, BD Bioscience) directly into 500 µL TRIzol (Invitrogen 15596026). The samples were stored at −80°C until they were shipped on dry ice. Total RNA extraction, library preparation, and sequencing were conducted by the Transcriptome and Genome Analysis Laboratory, University of Göttingen. Data were normalized and statistically analyzed using the DESeq2 algorithm (Love et al. 2014).

Statistical analysis

All statistical analyses and visualizations were performed using GraphPad Prism 10, with a significance level set at $\alpha = 0.05$. For normally distributed data, parametric statistical tests were used, and for nonnormally distributed data, nonparametric tests were used throughout. To compare individual groups against the level of chance, we used Holm–Sidak-corrected, two-tailed, one-sample *t*-tests for normally distributed data (as determined by the Shapiro–Wilk test), and Holm–Sidak-corrected, two-tailed, Wilcoxon signed-rank tests for nonparametric data. Parametric statistics were used for statistical analyses between groups that met the assumptions of a normal distribution (as determined by the Shapiro–Wilk test) and homogeneity of variance (as determined by Bartlett's test). Specifically, an unpaired *t*-test was used for comparisons between two groups, and a one-way ANOVA followed by planned pairwise comparisons using Tukey honestly significant difference (HSD) post hoc tests was conducted for comparisons among more than two groups. In cases where the data significantly deviated from the assumptions of normality and homogeneity of variance, nonparametric tests were used. The Mann–Whitney *U*-test was used for comparisons between two groups, and the Kruskal–Wallis test was used for comparisons among more than two groups. Dunn's multiple pairwise comparisons were performed post hoc, after the Kruskal–Wallis test. Detailed information on the specific statistical tests used, sample sizes, and descriptive statistics can be found in Supplemental Tables S1–S4 for the main figures and in Supplemental Figures. To assess the survival of flies under different feeding conditions, a Kaplan–Meier survival analysis was conducted. Significant differences between groups were analyzed using a Holm–Sidak-corrected log-rank test (Mantel–Cox).

Acknowledgments

We thank Clare E. Hancock, Ko-Eun Huh, Utku Ergün, and Marieke Theil for experimental assistance, Jochen Staiger for support with neuroanatomical data analysis, Bader Al-Anzi for the fly food recipes, and Oded Mayseless for helpful comments on the manuscript. We are also grateful to Gabriela Salinas and Emre Taylan Duman (NGS [Next-Generation Sequencing] Integrative Genomics Core Unit [NIG], University Medical Center Göttingen) for carrying out the RNA sequencing, and to Hiromu Tanimoto, the Bloomington stock center, and the Janelia Research Campus for providing *Drosophila* strains. This work was supported by the German Research Council through the CRC 889/B04 (project number 154113120) and the Research Unit FOR 2705 (project number 365082554), and by the Ministry of Science and Culture of Lower Saxony (project number ZN3014).

References

Al-Anzi B, Zinn K. 2018. Identification and characterization of mushroom body neurons that regulate fat storage in *Drosophila*. *Neural Dev* **13:** 18. doi:10.1186/s13064-018-0116-7

Alyagor I, Berkun V, Keren-Shaul H, Marmor-Kollet N, David E, Mayseless O, Issman-Zecharya N, Amit I, Schuldiner O. 2018. Combining developmental and perturbation-seq uncovers transcriptional modules orchestrating neuronal remodeling. *Dev Cell* **47:** 38–52.e6. doi:10.1016/j.devcel.2018.09.013

Aso Y, Herb A, Ogueta M, Siwanowicz I, Templier T, Friedrich AB, Ito K, Scholz H, Tanimoto H. 2012. Three dopamine pathways induce aversive odor memories with different stability. *PLoS Genet* **8:** e1002768. doi:10.1371/journal.pgen.1002768

Aso Y, Sitaraman D, Ichinose T, Kaun KR, Vogt K, Belliart-Guérin G, Plaçais PY, Robie AA, Yamagata N, Schnaitmann C, et al. 2014a. Mushroom body output neurons encode valence and guide memory-based action selection in *Drosophila*. *Elife* **3:** e04580. doi:10.7554/eLife.04580

Aso Y, Hattori D, Yu Y, Johnston RM, Iyer NA, Ngo TT, Dionne H, Abbott L, Axel R, Tanimoto H, et al. 2014b. The neuronal architecture of the mushroom body provides a logic for associative learning. *Elife* **3:** e04577. doi:10.7554/eLife.04577

Baltruschat L, Prisco L, Ranft P, Lauritzen JS, Fiala A, Bock DD, Tavosanis G. 2021. Circuit reorganization in the *Drosophila* mushroom body calyx accompanies memory consolidation. *Cell Rep* **34:** 108871. doi:10.1016/j.celrep.2021.108871

Benoit SC, Davis JF, Davidson TL. 2010. Learned and cognitive controls of food intake. *Brain Res* **1350:** 71–76. doi:10.1016/j.brainres.2010.06.009

Bilz F, Geurten BRH, Hancock CE, Widmann A, Fiala A. 2020. Visualization of a distributed synaptic memory code in the *Drosophila* brain. *Neuron* **106:** 963–976.e4. doi:10.1016/j.neuron.2020.03.010

Boehm AC, Friedrich AB, Hunt S, Bandow P, Siju KP, De Backer JF, Claussen J, Link MH, Hofmann TF, Dawid C, et al. 2022. A dopamine-gated learning circuit underpins reproductive state-dependent odor preference in *Drosophila* females. *Elife* **11:** e77643. doi:10.7554/eLife.77643

Boto T, Stahl A, Tomchik SM. 2020. Cellular and circuit mechanisms of olfactory associative learning in *Drosophila*. *J Neurogenet* **34:** 36–46. doi:10.1080/01677063.2020.1715971
Busto GU, Cervantes-Sandoval I, Davis RL. 2010. Olfactory learning in *Drosophila*. *Physiology* **25:** 338–346. doi:10.1152/physiol.00026.2010
Cervantes-Sandoval I, Phan A, Chakraborty M, Davis RL. 2017. Reciprocal synapses between mushroom body and dopamine neurons form a positive feedback loop required for learning. *Elife* **6:** e23789. doi:10.7554/eLife.23789
Cohn R, Morantte I, Ruta V. 2015. Coordinated and compartmentalized neuromodulation shapes sensory processing in *Drosophila*. *Cell* **163:** 1742–1755. doi:10.1016/j.cell.2015.11.019
Crittenden JR, Skoulakis EM, Han KA, Kalderon D, Davis RL. 1998. Tripartite mushroom body architecture revealed by antigenic markers. *Learn Mem* **5:** 38–51. doi:10.1101/lm.5.1.38
Davidson TL, Sample CH, Swithers SE. 2014. An application of Pavlovian principles to the problems of obesity and cognitive decline. *Neurobiol Learn Mem* **108:** 172–184. doi:10.1016/j.nlm.2013.07.014
Davis RL. 1993. Mushroom bodies and *Drosophila* learning. *Neuron* **11:** 1–14. doi:10.1016/0896-6273(93)90266-T
de Tredern E, Rabah Y, Pasquer L, Minatchy J, Plaçais PY, Preat T. 2021. Glial glucose fuels the neuronal pentose phosphate pathway for long-term memory. *Cell Rep* **36:** 109620. doi:10.1016/j.celrep.2021.109620
Driscoll M, Buchert SN, Coleman V, McLaughlin M, Nguyen A, Sitaraman D. 2021. Compartment specific regulation of sleep by mushroom body requires GABA and dopaminergic signaling. *Sci Rep* **11:** 20067. doi:10.1038/s41598-021-99531-2
Durst C, Eichmüller S, Menzel R. 1994. Development and experience lead to increased volume of subcompartments of the honeybee mushroom body. *Behav Neural Biol* **62:** 259–263. doi:10.1016/S0163-1047(05)80025-1
Eschment M, Franz HR, Güllü N, Hölscher LG, Huh KE, Widmann A. 2020. Insulin signaling represents a gating mechanism between different memory phases in *Drosophila* larvae. *PLoS Genet* **16:** e1009064. doi:10.1371/journal.pgen.1009064
Estes PS, Roos J, van der Bliek A, Kelly RB, Krishnan KS, Ramaswami M. 1996. Traffic of dynamin within individual *Drosophila* synaptic boutons relative to compartment-specific markers. *J Neurosci* **16:** 5443–5456. doi:10.1523/JNEUROSCI.16-17-05443.1996
Feinberg EH, Vanhoven MK, Bendesky A, Wang G, Fetter RD, Shen K, Bargmann CI. 2008. GFP Reconstitution Across Synaptic Partners (GRASP) defines cell contacts and synapses in living nervous systems. *Neuron* **57:** 353–363. doi:10.1016/j.neuron.2007.11.030
Fiala A. 2007. Olfaction and olfactory learning in *Drosophila*: recent progress. *Curr Opin Neurobiol* **17:** 720–726. doi:10.1016/j.conb.2007.11.009
Friggi-Grelin F, Coulom H, Meller M, Gomez D, Hirsh J, Birman S. 2003. Targeted gene expression in *Drosophila* dopaminergic cells using regulatory sequences from tyrosine hydroxylase. *J Neurobiol* **54:** 618–627. doi:10.1002/neu.10185
Garg V, André S, Giraldo D, Heyer L, Göpfert MC, Dosch R, Geurten BH. 2022. A markerless pose estimator applicable to limbless animals. *Front Behav Neurosci* **16:** 819146. doi:10.3389/fnbeh.2022.819146
Gerber B, Tanimoto H, Heisenberg M. 2004. An engram found? Evaluating the evidence from fruit flies. *Curr Opin Neurobiol* **14:** 737–744. doi:10.1016/j.conb.2004.10.014
Golic KG. 1991. Site-specific recombination between homologous chromosomes in *Drosophila*. *Science* **252:** 958–961. doi:10.1126/science.2035025
Gordon MD, Scott K. 2009. Motor control in a *Drosophila* taste circuit. *Neuron* **61:** 373–384. doi:10.1016/j.neuron.2008.12.033
Govorunova EG, Sineshchekov OA, Janz R, Liu X, Spudich JL. 2015. Natural light-gated anion channels: a family of microbial rhodopsins for advanced optogenetics. *Science* **349:** 647–650. doi:10.1126/science.aaa7484
Groh C, Lu Z, Meinertzhagen IA, Rössler W. 2012. Age-related plasticity in the synaptic ultrastructure of neurons in the mushroom body calyx of the adult honeybee *Apis mellifera*. *J Comp Neurol* **520:** 3509–3527. doi:10.1002/cne.23102
Grunwald Kadow IC. 2019. State-dependent plasticity of innate behavior in fruit flies. *Curr Opin Neurobiol* **54:** 60–65. doi:10.1016/j.conb.2018.08.014
Hancock CE, Rostami V, Rachad EY, Deimel SH, Nawrot MP, Fiala A. 2022. Visualization of learning-induced synaptic plasticity in output neurons of the *Drosophila* mushroom body γ-lobe. *Sci Rep* **12:** 10421. doi:10.1038/s41598-022-14413-5
Heisenberg M. 2003. Mushroom body memoir: from maps to models. *Nat Rev Neurosci* **4:** 266–275. doi:10.1038/nrn1074
Hergarden AC, Tayler TD, Anderson DJ. 2012. Allatostatin-A neurons inhibit feeding behavior in adult *Drosophila*. *Proc Natl Acad Sci* **109:** 3967–3972. doi:10.1073/pnas.1200778109
Hige T, Aso Y, Modi MN, Rubin GM, Turner GC. 2015. Heterosynaptic plasticity underlies aversive olfactory learning in *Drosophila*. *Neuron* **88:** 985–998. doi:10.1016/j.neuron.2015.11.003
Hirano Y, Masuda T, Naganos S, Matsuno M, Ueno K, Miyashita T, Horiuchi J, Saitoe M. 2013. Fasting launches CRTC to facilitate long-term memory formation in *Drosophila*. *Science* **339:** 443–446. doi:10.1126/science.1227170
Holtmaat A, Svoboda K. 2009. Experience-dependent structural synaptic plasticity in the mammalian brain. *Nat Rev Neurosci* **10:** 647–658. doi:10.1038/nrn2699
Honegger KS, Campbell RA, Turner GC. 2011. Cellular-resolution population imaging reveals robust sparse coding in the *Drosophila* mushroom body. *J Neurosci* **31:** 11772–11785. doi:10.1523/JNEUROSCI.1099-11.2011
Hourcade B, Muenz TS, Sandoz JC, Rössler W, Devaud JM. 2010. Long-term memory leads to synaptic reorganization in the mushroom bodies: a memory trace in the insect brain? *J Neurosci* **30:** 6461–6465. doi:10.1523/JNEUROSCI.0841-10.2010
Ito K, Suzuki K, Estes P, Ramaswami M, Yamamoto D, Strausfeld NJ. 1998. The organization of extrinsic neurons and their implications in the functional roles of the mushroom bodies in *Drosophila melanogaster Meigen*. *Learn Mem* **5:** 52–77. doi:10.1101/lm.5.1.52
Itskov PM, Moreira JM, Vinnik E, Lopes G, Safarik S, Dickinson MH, Ribeiro C. 2014. Automated monitoring and quantitative analysis of feeding behaviour in *Drosophila*. *Nat Commun* **5:** 4560. doi:10.1038/ncomms5560
Ja WW, Carvalhio GB, Mak EM, de la Rosa NN, Fang AY, Liong JC, Brummel T, Benzer S. 2007. Prandiology of *Drosophila* and the CAFE assay. *Proc Natl Acad Sci* **104:** 8253–8256. doi:10.1073/pnas.0702726104
Joiner WJ, Crocker A, White BH, Sehgal A. 2006. Sleep in *Drosophila* is regulated by adult mushroom bodies. *Nature* **441:** 757–760. doi:10.1038/nature04811
Josselyn SA, Tonegawa S. 2020. Memory engrams: recalling the past and imagining the future. *Science* **367:** eaaw4325. doi:10.1126/science.aaw4325
Kandel ER, Dudai Y, Mayford MR. 2014. The molecular and systems biology of memory. *Cell* **157:** 163–186. doi:10.1016/j.cell.2014.03.001
Kaun KR, Rothenfluh A. 2017. Dopaminergic rules of engagement for memory in *Drosophila*. *Curr Opin Neurobiol* **43:** 56–62. doi:10.1016/j.conb.2016.12.011
Kitamoto T. 2001. Conditional modification of behavior in *Drosophila* by targeted expression of a temperature-sensitive shibire allele in defined neurons. *J Neurobiol* **47:** 81–92. doi:10.1002/neu.1018
Klapoetke NC, Murata Y, Kim SS, Pulver SR, Birdsey-Benson A, Cho YK, Morimoto TK, Chuong AS, Carpenter EJ, Tian Z, et al. 2014. Independent optical excitation of distinct neural populations. *Nat Methods* **11:** 338–346. doi:10.1038/nmeth.2836
Kremer MC, Christiansen F, Leiss F, Paehler M, Knapek S, Andlauer TF, Förstner F, Kloppenburg P, Sigrist SJ, Tavosanis G. 2010. Structural long-term changes at mushroom body input synapses. *Curr Biol* **20:** 1938–1944. doi:10.1016/j.cub.2010.09.060
Larsen MJ, Burton KJ, Zantello MR, Smith VG, Lowery DL, Kubiak TM. 2001. Type A allatostatins from *Drosophila melanogaster* and *Diplotera puncata* activate two *Drosophila* allatostatin receptors, DAR-1 and DAR-2, expressed in CHO cells. *Biochem Biophys Res Commun* **286:** 895–901. doi:10.1006/bbrc.2001.5476
Lee T, Luo L. 1999. Mosaic analysis with a repressible cell marker for studies of gene function in neuronal morphogenesis. *Neuron* **22:** 451–461. doi:10.1016/S0896-6273(00)80701-1
Liu C, Plaçais PY, Yamagata N, Pfeiffer BD, Aso Y, Friedrich AB, Siwanowicz I, Rubin GM, Preat T, Tanimoto H. 2012. A subset of dopamine neurons signals reward for odour memory in *Drosophila*. *Nature* **488:** 512–516. doi:10.1038/nature11304
Lövdén M, Wenger E, Mårtensson J, Lindenberger U, Bäckman L. 2013. Structural brain plasticity in adult learning and development. *Neurosci Biobehav Rev* **37:** 2296–2310. doi:10.1016/j.neubiorev.2013.02.014
Love MI, Huber W, Anders S. 2014. Moderated estimation of fold change and dispersion for RNA-seq data with DESeq2. *Genome Biol* **15:** 550. doi:10.1186/s13059-014-0550-8
MacPherson LJ, Zaharieva EE, Kearney PJ, Alpert MH, Lin TY, Turan Z, Lee CH, Gallio M. 2015. Dynamic labelling of neural connections in multiple colours by trans-synaptic fluorescence complementation. *Nat Commun* **6:** 10024. doi:10.1038/ncomms10024
Maleszka J, Barron AB, Helliwell PG, Maleszka R. 2009. Effect of age, behaviour and social environment on honey bee brain plasticity. *J Comp Physiol A* **195:** 733–740. doi:10.1007/s00359-009-0449-0
Martelli C, Pech U, Kobbenbring S, Pauls D, Bahl B, Sommer MV, Pooryasin A, Barth J, Arias CWP, Vassiliou C, et al. 2017. SIFamide translates hunger signals into appetitive and feeding behavior in *Drosophila*. *Cell Rep* **20:** 464–478. doi:10.1016/j.celrep.2017.06.043

Masuyama K, Zhang Y, Rao Y, Wang JW. 2012. Mapping neural circuits with activity-dependent nuclear import of a transcription factor. *J Neurogenet* **26:** 89–102. doi:10.3109/01677063.2011.642910
Menzel R. 2022. In search for the retrievable memory trace in an insect brain. *Front Syst Neurosci* **16:** 876376. doi:10.3389/fnsys.2022.876376
Neumüller RA, Betschinger J, Fischer A, Bushati N, Poernbacher I, Mechtler K, Cohen SM, Knoblich JA. 2008. Mei-P26 regulates microRNAs and cell growth in the *Drosophila* ovarian stem cell lineage. *Nature* **454:** 241–245. doi:10.1038/nature07014
Owald D, Felsenberg J, Talbot CB, Das G, Perisse E, Huetteroth W, Waddell S. 2015. Activity of defined mushroom body output neurons underlies learned olfactory behavior in *Drosophila*. *Neuron* **86:** 417–427. doi:10.1016/j.neuron.2015.03.025
Pardo-Garcia TR, Gu K, Woerner RKR, Dus M. 2023. Food memory circuits regulate eating and energy balance. *Curr Biol* **33:** 215–227.e3. doi:10.1016/j.cub.2022.11.039
Park S, Sonn JY, Oh Y, Lim C, Choe J. 2014. SIFamide and SIFamide receptor defines a novel neuropeptide signaling to promote sleep in *Drosophila*. *Mol Cells* **37:** 295–301. doi:10.14348/molcells.2014.2371
Pavlov IP. 1927. *Conditioned reflexes: an investigation of the physiological activity of the cerebral cortex*. Oxford University Press, London.
Pech U, Pooryasin A, Birman S, Fiala A. 2013. Localization of the contacts between Kenyon cells and aminergic neurons in the *Drosophila melanogaster* brain using SplitGFP reconstitution. *J Comp Neurol* **521:** 3992–4026. doi:10.1002/cne.23388
Pech U, Revelo NH, Seitz KJ, Rizzoli SO, Fiala A. 2015. Optical dissection of experience-dependent pre- and postsynaptic plasticity in the *Drosophila* brain. *Cell Rep* **10:** 2083–2095. doi:10.1016/j.celrep.2015.02.065
Plaçais PY, de Tredern É, Scheunemann L, Trannoy S, Goguel V, Han KA, Isabel G, Preat T. 2017. Upregulated energy metabolism in the *Drosophila* mushroom body is the trigger for long-term memory. *Nat Commun* **8:** 15510. doi:10.1038/ncomms15510
Qin H, Cressy M, Li W, Coravos JS, Izzi SA, Dubnau J. 2012. γ Neurons mediate dopaminergic input during aversive olfactory memory formation in *Drosophila*. *Curr Biol* **22:** 608–614. doi:10.1016/j.cub.2012.02.014
Riemensperger T, Völler T, Stock P, Buchner E, Fiala A. 2005. Punishment prediction by dopaminergic neurons in *Drosophila*. *Curr Biol* **15:** 1953–1960. doi:10.1016/j.cub.2005.09.042
Sayin S, De Backer JF, Siju KP, Wosniack ME, Lewis LP, Frisch LM, Gansen B, Schlegel P, Edmondson-Stait A, Sharifi N, et al. 2019. A neural circuit arbitrates between persistence and withdrawal in hungry *Drosophila*. *Neuron* **104:** 544–558.e6. doi:10.1016/j.neuron.2019.07.028
Scaplen KM, Talay M, Fisher JD, Cohn R, Sorkaç A, Aso Y, Barnea G, Kaun KR. 2021. Transsynaptic mapping of *Drosophila* mushroom body output neurons. *Elife* **10:** e63379. doi:10.7554/eLife.63379
Schindelin J, Arganda-Carreras I, Frise E, Kaynig V, Longair M, Pietzsch T, Preibisch S, Rueden C, Saalfeld S, Schmid B, et al. 2012. Fiji: an open-source platform for biological-image analysis. *Nat Methods* **9:** 676–682. doi:10.1038/nmeth.2019
Schwaerzel M, Heisenberg M, Zars T. 2002. Neuron extinction antagonizes olfactory memory at the subcellular level. *Neuron* **35:** 951–960. doi:10.1016/S0896-6273(02)00832-2
Senapati B, Tsao CH, Juan YA, Chiu TH, Wu CL, Waddell S, Lin S. 2019. A neural mechanism for deprivation state-specific expression of relevant memories in *Drosophila*. *Nat Neurosci* **22:** 2029–2039. doi:10.1038/s41593-019-0515-z
Sitaraman D, Aso Y, Jin X, Chen N, Felix M, Rubin GM, Nitabach MN. 2015. Propagation of homeostatic sleep signals by segregated synaptic microcircuits of the *Drosophila* mushroom body. *Curr Biol* **25:** 2915–2927. doi:10.1016/j.cub.2015.09.017
Stahl A, Noyes NC, Boto T, Botero V, Broyles CN, Jing M, Zeng J, King LB, Li Y, Davis RL, et al. 2022. Associative learning drives longitudinally graded presynaptic plasticity of neurotransmitter release along axonal compartments. *Elife* **11:** e76712. doi:10.7554/eLife.76712
Steinman MQ, Gao V, Alberini CM. 2016. The role of lactate-mediated metabolic coupling between astrocytes and neurons in long-term memory formation. *Front Integr Neurosci* **10:** 10. doi:10.3389/fnint.2016.00010
Stierl M, Stumpf P, Udwari D, Gueta R, Hagedorn R, Losi A, Gärtner W, Petereit L, Efetova M, Schwärzel M, et al. 2011. Light modulation of cellular cAMP by a small bacterial photoactivated adenylyl cyclase, bPAC, of the soil bacterium Beggiatoa. *J Biol Chem* **286:** 1181–1188. doi:10.1074/jbc.M110.185496
Suzuki A, Stern SA, Bozdagi O, Huntley GW, Walker RH, Magistretti PJ, Alberini CM. 2011. Astrocyte-neuron lactate transport is required for long-term memory formation. *Cell* **144:** 810–823. doi:10.1016/j.cell.2011.02.018
Talhati F, Patti CL, Zanin KA, Lopes-Silva LB, Ceccon LM, Hollais AW, Bizerra CS, Santos R, Tufik S, Frussa-Filho R. 2014. Food restriction increases long-term memory persistence in adult or aged mice. *Prog Neuropsychopharmacol Biol Psychiatry* **50:** 125–136. doi:10.1016/j.pnpbp.2013.12.007
Tanaka NK, Tanimoto H, Ito K. 2008. Neuronal assemblies of the *Drosophila* mushroom body. *J Comp Neurol* **508:** 711–755. doi:10.1002/cne.21692
Tempel BL, Bonini N, Dawson DR, Quinn WG. 1983. Reward learning in normal and mutant *Drosophila*. *Proc Natl Acad Sci* **80:** 1482–1486. doi:10.1073/pnas.80.5.1482
Thévenaz P, Ruttimann UE, Unser M. 1998. A pyramid approach to subpixel registration based on intensity. *IEEE Trans Image Process Publ* **7:** 27–41. doi:10.1109/83.650848
Tsao CH, Chen CC, Lin CH, Yang HY, Lin S. 2018. *Drosophila* mushroom bodies integrate hunger and satiety signals to control innate food-seeking behavior. *Elife* **7:** e35264. doi:10.7554/eLife.35264
Tully T, Quinn WG. 1985. Classical conditioning and retention in normal and mutant *Drosophila melanogaster*. *J Comp Physiol A*. **157:** 263–277. doi:10.1007/BF01350033
Turner GC, Bazhenov M, Laurent G. 2008. Olfactory representations by *Drosophila* mushroom body neurons. *J Neurophysiol* **99:** 734–746. doi:10.1152/jn.01283.2007
Wang L, Wu C, Peng W, Zhou Z, Zeng J, Li X, Yang Y, Yu S, Zou Y, Huang M. 2022. A high-performance genetically encoded fluorescent indicator for in vivo cAMP imaging. *Nat Commun* **13:** 5363. doi:10.1038/s41467-022-32994-7
Withers GS, Fahrbach SE, Robinson GE. 1993. Selective neuroanatomical plasticity and division of labour in the honeybee. *Nature* **364:** 238–240. doi:10.1038/364238a0
Yamada D, Davidson AM, Hige T. 2024. Cyclic nucleotide-induced bidirectional long-term synaptic plasticity in *Drosophila* mushroom body. *J Physiol* **602:** 2019–2045. doi:10.1113/JP285745
Yamagata N, Hiroi M, Kondo S, Abe A, Tanimoto H. 2016. Suppression of dopamine neurons mediates reward. *PLoS Biol* **14:** e1002586. doi:10.1371/journal.pbio.1002586
Zars T, Fischer M, Schulz R, Heisenberg M. 2000. Localization of a short-term memory in *Drosophila*. *Science* **288:** 672–675. doi:10.1126/science.288.5466.672

Received January 29, 2024; accepted in revised form April 10, 2024.